

AL- MUHANDIS

Journal (JMISE)

Established in 1956

ISSN 2413 - 0230

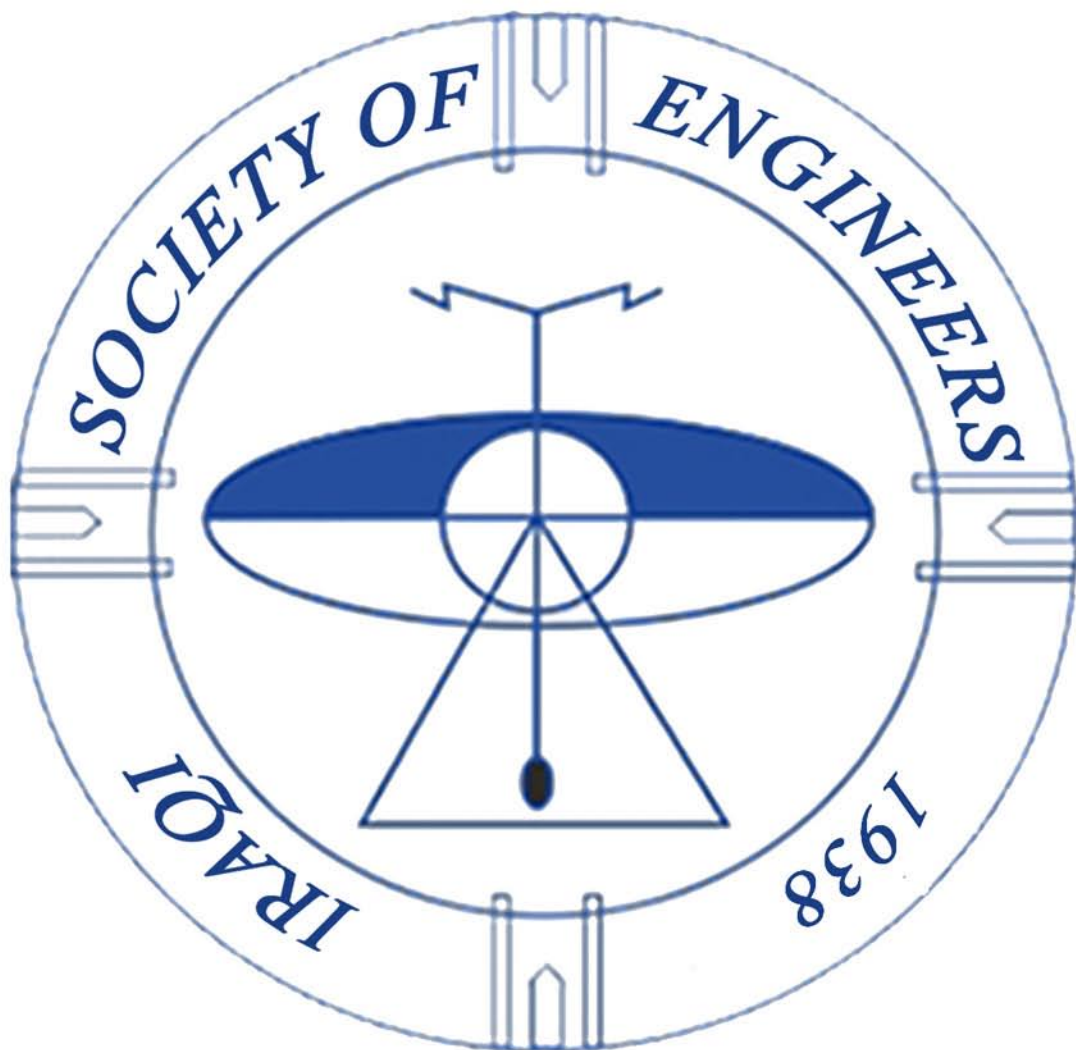
Volume 155, Issue 3, September 2018

Peer-Reviewed Scientific Journal

Published by

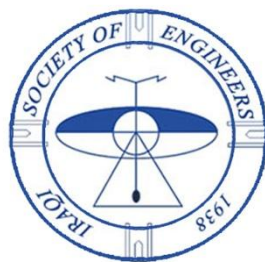
Iraqi Society of Engineers (ISE)

Founded in 1938



Al-MUHANDIS Journal (JMISE)

Volume 155, Issue 3, September 2018



Iraqi Society of Engineers

Publication Information

Al-MUHANDIS Journal (JMISE) is a seasonal scientific publication releases by the Iraqi Society of Engineers (ISE) as a hard copy as well as online. The journal has established for the first time in 1956.

ISSN: 2413-0230

Copyright © 2018 by Iraqi Society of Engineers (ISE)

Office Address: Iraq, Baghdad, Al-Nidhal Q., 103-30-5

P.O. Box: 18429

Mob: (+964) 7702526721 / (+964) 7901151092 / (+964) 7901803967

Online: www.jmise.ise-iq.org

E-mail: jmise@ise-iq.org

Subscription: 100000 ID Per Year in Iraq

\$600 per year for other countries

Aims and Scope

Al-MUHANDIS Journal (JMISE) is a peer-reviewed scientific journal, covers all sorts of scientific researches in many engineering fields like: Civil and Construction, Architectural, Mechanical, Electrical, Communications, Computer, Chemical, Petroleum, Environmental, Materials, Water Resources as well as other engineering interests. The journal offers a solid platform for Iraqi engineers to publish works which translate their knowledge, expertise and skills.

Publication Ethics

The journal accepts the submission of any research work deals with engineering fields, either methodology and/or applications. Prospective authors are invited to submit their draft manuscript in a short paper (no more than 15 pages) using MS Word format. The manuscripts should be processed through many steps in order to get acceptance. These processes are:

- Authorship satisfaction
- Standards validation
- Plagiarism complaints
- Anti- duplicate publication
- Anti- misappropriation
- Malpractice statement
- Readable for international audiences (at least titles and abstracts in English).
- Peer reviewing
- Editorial acceptance

The target is that the process for each submitted manuscript should complete within (10) weeks from its submission. All papers should include: (1) Name of the journal, (2) Title of the manuscript, (3) Name and affiliation for the author(s); (4) Abstract; (5) Keywords; (6) Text of the manuscript; (7) References.

Iraqi Society of Engineers

Iraqi society of engineers (ISE) has founded in 1938 by a group of leading Iraqi engineers. ISE has been assigned 36 administration commissions since its formation up to date. The number of members has been grown up from several members during its declaration to more than 4,000 members recently. ISE has several committees and boards to operate scientific, engineering and cultural activities continuously in order to support Iraqi engineers by the required expertise and skills. ISE has a number of activities aimed to satisfy their goals by:

1. Establishment of scientific conferences, symposia and events.
2. Establishment continuous education courses and workshops.
3. Organizing scientific publications, lectures and platforms.
4. Supporting scientific studies and researches.
5. Organizing scientific visits.
6. Collecting scientific documents and data bases for engineering purposes.
7. providing expertise and engineering consultancy.

Administration Commission

- Consultant Engineer Falih Kadhim Zayer\ President of ISE& administration chairman
- Prof. Dr. Hussein Yousif Mahmood\ Vice President of ISE
- Consultant Engineer Ali H.Al-allaq\ Administrative Board of ISE
- Engineer Mohammed Farooq Abdul-khaleq\ Treasurer of ISE
- Asst. Prof. Dr. Maher Yahya Sallom
- Dr. Falih Hamzah Al-Rubyei
- Dr. Hayder Amer Al-Baghdadi
- Asst. Lecturer Ahmed Saleh Al-Zuhairi
- Consultant Engineer Riadh Katab Husain
- Consultant Engineer Hamodi Kadeer Mohammed
- Consultant Engineer Abdel Salam A. Issa
- Engineer Abdul-lateef H. Sankoor

Editorial Board

- Prof. Dr. Hussein Yousif Mahmood\ Editor-in-chief
University of Baghdad, College of Engineering
- Prof. Dr. Najdet Nashat Abdullah
Al-Farabi University, College of Engineering
- Prof. Dr. Mohammed Z. Al Faiz
Nahrain University, College of Engineering
- Prof. Dr. Ghada Mousa Rzoki
University of Baghdad, College of Engineering
- Prof. Maher K. Mahmood Al Azawi
Al-Mustansiriyah University, College of Engineering
- Asst. Prof. Dr. Samira M. Hamdullah
University of Baghdad, College of Engineering
- Asst. Prof. Dr. Ahmed Zaidan Mohammed Shammari
University of Baghdad, Al-Khwarizmi College of Engineering
- Asst. Prof. Dr. Naseer A. Al-Haboubi
Nahrain University, College of Engineering
- Asst. Prof. Dr. Maan Salman Hassan
University of Technology, Civil Engineering Dept.
- Lecturer Dr. Ameer Mohammed Rahman Al-Mayah
University of Baghdad, Al-Khwarizmi College of Engineering
- Lecturer Dr. Tawfeeq Wasmi Mohammed
Al-Mustansiriyah University, College of Engineering

Advisors

- Prof. Dr. Ameen Daway Thamir\ Head of University of Technology
- Prof. Dr. Majid H. Majeed\ Head of Middle Technical University
- Prof. Dr. Mudaffar S. Al-Zuhairy\ Head of Southern Technical University
- Prof. Dr. Kasim J. Slaiman\ Professor in chemical Engineering
- Prof. Dr. Rami Hikmat Fouad Al-Hadeethi\ Professor in University of Jordan
- Prof. Dr. Ihsan Fethi\ Professor in Architectural Engineering in Denmark
- Prof. Dr. Khalid Al-Sultany\ Professor in Architectural Engineering in USA

Contents

- The parameters which effect material removal for rotation work piece in chemical machining process of Titanium alloy** 7-12
Dunia Adnan Ghullam, Assistant Professor Abbas Fadhil Ibrahim
- Effect of Spot Cooling System on the Human Thermal Comfort** 13-22
Ahmed J. Khaleel
- Applying a quality improvement program in local industry** 23-33
Tariq M. Ali
- Measurement of Residual Stresses of Al/Mg Compounds by the Hole Drilling Strain Gage Method with MATLAB Package(RSHDM)** 34-49
Ass. Prof. Dr. Abdullah Dhayea Assi , Lecturer Dr.Safaa M. Hassoni
Lecturer Ahmed Jasim Mohammed , Lecturer Ameer H. Sabry
- Effect of Dipping Time and temperature on Produced Intermetallic Phases thickness in Hot Dip Galvanizing Process** 50-58
BsC. Ruba Hussain Eleue / Asst. Prof. PhD. Bahaa S. Mahdi

The parameters which effect material removal for rotation work piece in chemical machining process of Titanium alloy

Dunia Adnan Ghullam ¹, Assistant Professor Abbas Fadhil Ibrahim ²

^{1,2} Department of Production Engineering and Metallurgy, University of Technology, Baghdad, Iraq.

ABSTRACT

The material removal in the chemical milling process which is one of the nonconventional operations happen when the machined work part will be in contact with active etchant solution. The aim of this research is studying the effect of chemical milling machining parameters (machining duration, the concentration and the temperature of the used etchant) on material removal when using rotation work piece technique for titanium alloy as a machined samples. Two different concentration for the etchant used in this research the quantities of the first one are (6 %HF, 10 %HNO₃ in 84 %H₂O) the quantities of the second one are (10 %HF, 15 %HNO₃ in 75 %H₂O), eight samples used in this research with dimensions of (30 * 10 * 1) mm, four levels of machining duration were used (4, 6, 8 and 10) min also four levels of machining temperatures were used (35, 40, 45 and 50) °C for both used etchant concentrations. The results showed that the material removal increased with the increasing of the time, temperature and the concentration of the used etchant for rotation work piece.

KEYWORDS

Chemical machining, Titanium, weight removal, etchant, parameters.

NOMENCLATURES

MR	material removal
t _m	machining time
T	machining temperature
HF	hydrofluoric acid
HNO ₃	nitric acid

ARTICLE INFO

Received 26 April 2018

Accepted 30 August 2018

DOI: 10.xxxxx

ISSN: 2413-0230

AL-MUHANDIS Journal (JMISE)

© 2018 Iraqi Society of Engineers (ISE)

E-mail: jmise@ise-iq.org

Online: www.ise-iq.org

Office Address: Iraq, Baghdad, Al-Nidhal Q., 103-30-5

CORRESPONDING AUTHOR

Name: Dunia Adnan Ghullam

Email: dunia.adnan9@yahoo.com

Research Field: production engineering\metals cutting.

INTRODUCTION:

The Chemical machining operations are a regular methods from the nonconventional machining methods in which a suitable active chemical etchant solution applies on the machined part to obtain a desired dimensions and eliminate undesirable metal from the machined work part by controlling the chemical etchant and the other used chemical machining parameters. Chemical machining operations widely used for manufacturing different types of sheets and it is used in electronics manufacture and in medical field industry. It also can produce complex shapes products with very high accuracy in dimensions and the material properties will not be affected with low machining duration and the cost of production process is very low compare with other nonconventional and conventional operations [1].

There are many parameters effect process efficiency one of the most important effective parameter is the etchant type and it's concentration, the other effective parameter is the maskant type and the way in which it applies on the machined work part, machining duration and the temperature of the etchant solution also have a large effect on the chemical machining process. The surface roughness, material removal rate and the toleration of the production are very effected by the direct influence of these parameters [2].

There are several kind of chemical machining operation. Chemical milling which is used in this research is one of the types of chemical machining operation and it is used for removing the material from all over the machined part, making pocket, and to contour the work part. Another kind is chemical blanking it is used to etch the thin sheet. To etch different types of metal in microelectronic products with photosensitive resist this can be carried out by using operation called photochemical machining operation. The etchant solution and maskant material are the most important used material in chemical milling operation. Etchant is an acid or alkaline solution the concentration and temperature must be under control during the operation. Maskant is an elastomer or polymer must be able to resist the used etchant during the machining process [3]. Maskant material is used to

protect the unwanted to etch areas of work part surface from chemical etchant. Polymers or rubbers based materials are commonly used for masking operation. There are many types of etchant, depending on the type of material to be etch an appropriate type of etchant will be selected from table (1) which represents different types of etchants which are used to machine different metals [4].

TABLE (1). TYPES OF CHEMICAL ETCHANTS FOR DIFFERENT MATERIALS

Materials	Chemical etchants	Concentration	Etching Temperature °C	Etch rate mm/min
Aluminum and alloys	FeCl ₃	(12-18°) Bé (*)	49	0.013-0.025
Copper and alloys	FeCl ₃ CuCl ₂ Alkaline etchants	(42°) Bé	49	2.0
		(35°) Bé	54	1.0
		---	50	---
Steel	FeCl ₃	(42°) Bé	54	0.025
Nickel	FeCl ₃	(42°) Bé	49	0.13-0.38
Magnesium	HNO ₃	(12-15)%	32-49	1.0
Titanium	HF	---	---	1.0
Glass	HF and HF+HNO ₃	---	---	---

*((The calculation of Baumé (Bé) value is $Bé = 145 (sg-1)/sg$)).

(Rui Neto, Teresa Duarte 2017) improved that when using a solution which consist of (4.5 %HF, 7.5 %HNO₃, 5 %Erkantol and 83 %H₂O) to chemically machine titanium aluminide can obtain higher material removal rate than the other used etchant [5]. (Matsuhashi, Kazuhiro Takahashi 2002) studied the effect of machining time, nitric acid (HNO₃) and hydrofluoric acid (HF) concentration on the corrosion loss of titanium. They found that any increasing in one of these parameters lead to increase in the corrosion loss of the machined titanium [6]. (Ho S. 2008) Showed that the rate of metal removal is up to six times greater for nanocrystalline Ni than conventional polycrystalline Ni and shorter working times are needed [7]. (David M. Allen 2004) improved that any change in etchant concentration and it's temperature have large effect on the etching rate and the dimensions of the etched part and the surface finish also affected by the changes [8].

EXPEREMENTAL PART:

In this research many materials were used. The alloy which used was titanium alloy and its chemical composition is shown in table (2). Polyester resin mixed with methyl ethyl ketone used as a maskant material. One side of the specimens to be machined coated with the maskant by using small brush. The etchant which is used in this research was a mixture of hydrofluoric acid (HF) with nitric acid (HNO₃) in

elements	Percentage	elements	percentage
Al	2.56%	Sn	Less than 0.0005%
V	Less than 0.0037%	Ni	0.031%
Cr	0.0283%	Si	0.031%
Cu	0.354%	Zr	0.0148%
Fe	0.106%	Pd	0.005%
Mn	1.28%	Ru	0.0233%
Mo	0.036%	W	Less than 0.01%
Nb	0.0519%	Ta	0.0484%

The remaining is Titanium and it is about 95.4161%

specific quantities.

TABLE (2). CHEMICAL COMPOSITION OF TITANIUM ALLOY

SAMPLES PREPARATION:

The dimensions of the used specimens in this research were (30*10*1) mm, a hole with (2.5) mm diameter was drilled by using drilling machine for ease carrying and submersing the machined samples, the maskant material applied on one side of the machined samples and the other side represents the working aria. The surface area of the samples was determined before coating them with the masking material, also the weight of all samples was recorded before the machining process to use it to calculate the material removal of the machined samples. Figure (1) represents one of the samples before and after coating it with the maskant material.

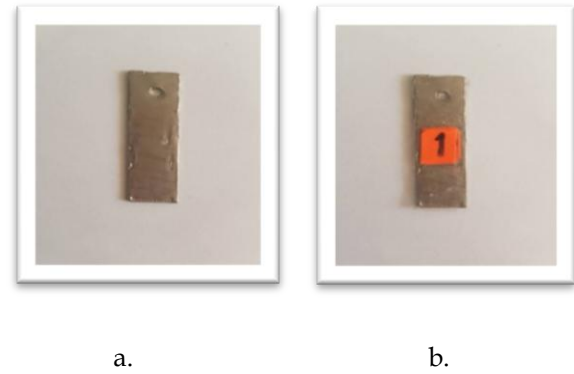


Figure 1. a. The sample before coating it with the maskant. b. The sample after coating it with the maskant.

Two different concentrations of etchant were used in this research. Acid concentration for the first was (16 %) the quantities of it was (6 % HF, 10 % HNO₃ in 84 % H₂O), acid concentration for the second etchant was (25 %) the quantities of it was (10 % HF, 15 % HNO₃ in 75 % H₂O), four levels of other machining parameters was used, the machining time levels was (4, 6, 8, 10) minute, the used temperature levels was (35, 40, 45, 50) degree centigrade the same time and temperature used with the both concentrations. Figure (3) represents the setup of the chemical milling process by using rotation work piece strategy.



Figure 3. Chemical machining setup for rotation work piece.

In this technique a small motor with (120) rpm was used to rotate the sample during the machining process and a stand to handle the sample and immerse it in to the beaker which contain the etchant solution and placed on a stirrer device

which is used to regulate the suitable machining temperature for each experiment of the eight carried out experiments. After the chemical milling process was carried out the samples will be wash very well with distilled water and dried also the maskant layer will be removed from the surface of the machined samples and the weighing of them will be recorded to detect the difference between the weight of the samples before and after the machining process to determine the material removal.

RESULTS AND DISCUSSION:

The material removal of the machined specimens was determined after measuring the difference between the weight of the specimens before and after the machining process and the surface area of each specimen, by applying equation (1).

$$\text{Material removal} = \frac{w_b - w_a}{A} \text{ mg/mm}^2 \quad (1)$$

W_b: represent the weight of the specimen before machining process (mg)

W_a: represent the weight of the specimen after machining process (mg)

A: represent the surface area of the specimen (mm²)

TABLE 3. MATERIAL REMOVAL OF THE MACHINED SPECIMENS.

No	W _b	T	t _m	Con.	W _o	ΔW	A	MR
1	1560	35	4	16	1470	90	384	0.2344
2	1160	40	6	16	1080	80	290	0.2759
3	1210	45	8	16	1080	130	305	0.4262
4	1310	50	10	16	1110	200	310	0.6452
5	1560	35	4	25	1470	90	372	0.2419
6	1240	40	6	25	1080	160	295	0.5424
7	1320	45	8	25	950	370	315	1.1746
8	1220	50	10	25	840	380	295	1.2881

t_m represents the machining time min.

T represents the machining temperature C°.

MR represents the material removal mg/mm².

ΔW represents the difference between the weight mg/mm².

By using response surface methodology (RSM) from Minitab 2018 program these data was analyzed, table (4) represents the analyzed material removal by (RSM).

TABLE 4. ANALYZED MATERIAL REMOVAL BY (RSM).

NO.	T (C°)	t _m (min)	con. %	MR (mg/mm ²)	Predicted MR (mg/mm ²)
1	35	4	16	0.2344	0.18802
2	40	6	16	0.2759	0.32629
3	45	8	16	0.4262	0.46456
4	50	10	16	0.6452	0.60283
5	35	4	25	0.2419	0.24613
6	40	6	25	0.5424	0.62321
7	45	8	25	1.1746	1.00029
8	50	10	25	1.2881	1.37737

Equation (2) represent the regression equation which is used to detect the predicted material removal.

$$\text{Predicted material removal} = 2.09 - 0.0573 * T - 0.1793 * \text{con.} + 0.00531 * T * \text{con.} \quad (2)$$

From equation (2) it is clear that the concentration has the largest effect on the predicted material removal.

From figure (4) which is represents the normal plot for the analyzed data of material removal by using (RSM) noted that the errors were normally distributed.

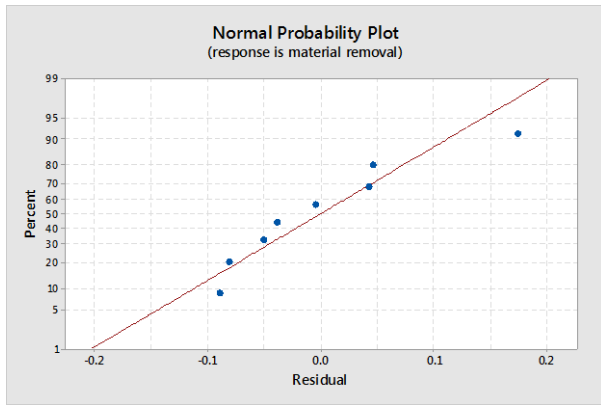


Figure 4. Material removal normal plot by (RSM).

ANALYSIS OF VARIANCE:

The analysis of variance (ANOVA) based on statistical purpose to make a decision for detecting the changes in the behavior of the analyzed group of data. According to these changes the decisions can be taken to detect which factor has the greatest effect than other used machining factors and how the design of experiment should be set [7]. Table (5) represents the analysis of variance for material removal by (RSM).

Table 5. (ANOVA) by (RSM).

Source	DF	Adj SS	Adj MS	F-value	P-value
Model	3	1.15319	0.38440	29.09	0.004
Linear	2	1.01062	0.50531	38.24	0.002
Temperature	1	0.66396	0.66396	50.24	0.002
Concentration	1	0.34665	0.34665	26.23	0.007
2-way Interaction	1	0.14258	0.14258	10.79	0.030
T*con.	1	0.14258	0.14258	10.79	0.030
Error	4	0.05286	0.01321	\	\
Total	7	1.20605	\	\	\

Where the degree of freedom was represented by DF, adjusted square of sum represented by Adj-SS and the adjusted square of means.

Table 5 showed that the temperature had the largest effect on material removal which was (50.24) the effect of concentration which was (26.23).

The model summary for the analyzing process was given in table (6).

TABLE 6. MODEL SUMMARY FOR ANALYSIS DATA.

S	R-sq	R-sq(adj)	R-sq(pred)
0.114955	95.62%	92.33%	82.08%

The ability of the independent parameters to predict the dependent parameters represented by R-sq.

THE EFFECT OF PARAMETERS ON MATERIAL REMOVAL FOR ROTATION WOK PIECE:

All the machining parameters have a large effect on material removal. When the rotation strategy was used to rotate the machined specimen a larger values of material removal were obtained than when same parameters was used for static sample. The temperature had the largest effect on the material removal. Figures bellow represent the effect of temperature and time on weight removal and these figures showed when any increasing happened in one of the used machining parameters (temperature, time, and concentration) lead to increase in the material removal. Figure (5) represents the effect of temperature and time on material removal for acid concentration (16) %. Figure (6) represents the effect of temperature and time on weight removal for acid concentration (25) %.

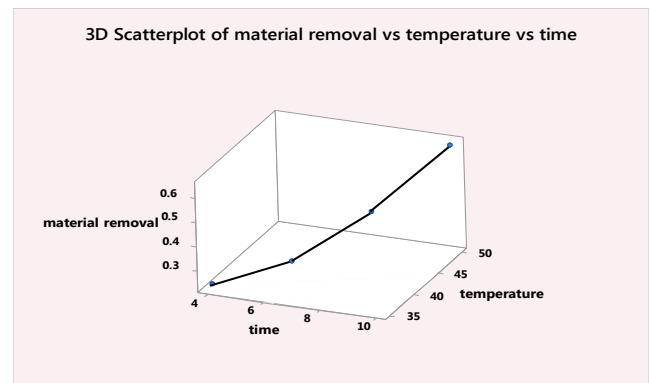


Figure 5. Effect of temperature and time on material removal at acid concentration 16 %.

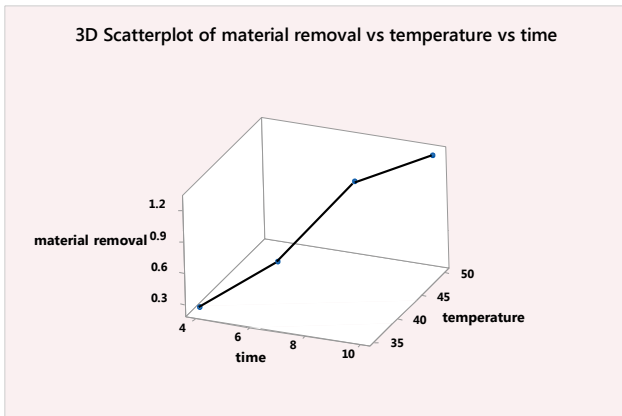


Figure 6. Effect of temperature and time on weight removal at concentration 25 %.

CONCLUSIONS:

1. We can get larger material removal by increasing one of the used machining parameters.
2. The value of coefficient of determination was very good it was (95.62) % that means the independent factors have a very good ability to predict the dependent factors by using response surface methodology.
3. The effect of temperature was larger than the effect of acid concentration. It was (50.24) for temperature and (26.23) for concentration according to analysis of variance table.
4. Rotation work piece strategy leads to obtain largest values of material removal than static work piece when using same machining parameters.

REFERENCES:

- [1] Orhan Çakır, "Chemical machining of cz128 copper alloy", Yildiz Technical University, Istanbul, Turkey, 2016.
- [2] Haydar A. H. Al-Ethari, Kadhim Fintee Al-Sultani, "Variables Affecting the Chemical Machining of Stainless Steel 420", International Journal of Engineering and Innovative Technology (IJEIT), Volume 3, Issue 6, December 2013.

[3] A. Fadaei Tehrani, E. Imanian "A new etchant for the chemical machining of St304" Journal of Materials Processing Technology 149 (2004) 404–408.

[4] O. Çakır, A. Yardımeden, "Chemical machining" Archives of Materials Science and Engineering, Volume 28, Issue 8, 2007.

[5] Rui Neto, Teresa Duarte "effect of chemical milling process on the surface of titanium aluminum castings" ciencia and tecnologia dos materiais 29 (2017) e40-e45.

[6] Roy Matsuhashi, Kazuhiro Takahashi "the integral rate equation of pure titanium in nitric hydrofluoric acid solutions" Nippon steel technical report no. 85 January 2002.

[7] Ho S., "Chemical Machining of Nanocrystalline Ni", Department of Materials Science and Engineering, University of Toronto, 184 College Street, Toronto, Canada 2008.

[8] David M. Allen, "Characterization of Aqueous Ferric Chloride Etchant Used in Industrial Photochemical Machining", School of Industrial and Manufacturing Science, Cranfield University, UK, 2004.

[9] N.D. Misal, "Optimization Of Process Parameters In Etching During Photo Chemical Machining Process" SVERIAN Scientific, Shri Vithal Education & Research Institute, Pandharpur, 473-484, 2005.

Effect of Spot Cooling System on the Human Thermal Comfort

Ahmed J. Khaleel

Technical Engineering College- Baghdad, Middle Technical University

ABSTRACT

An experimental investigation was carried out to study the air distribution indoor using a spot cooling system and its effect on the human thermal comfort. A room (L 4.8 m × W 3.8 m × H 3.8 m) has been set-up to provide an acceptable office environment. The initial indoor dry bulb temperature was 34°C in October 2016 at 2pm. An air distribution system was built and equipped with six air 40 mm diameter conduits. The influence of temperature and airflow fields on the human comfort level were studied experimentally on a personal space with dimensions (1m×1m×1.8m). The air velocity for all inlets was set from 1.2 - 2.4 m/s with air temperature supply ranged from 13.5 - 15.7 °C for case-1 and 1.2 - 1.8 m/s with air temperature from 13.3-16 °C for case-2. Two cases of air distribution were studied to reach the best possible method of cooling limited personal space within large zones thereby reduce energy consumption. For the case-1 the air was supplied in perpendicular and horizontal directions, while in the case-2 all air sources were fixed horizontally. The results showed that the case-2 has lower temperatures in some regions and same temperatures in other regions compared to case-1. The temperature distribution in the case-2 is more homogeneous than in the case-1. These will make the second method of air distribution more convenient for the comfort requirements of humans.

KEYWORDS

Spot, Air distribution, Air temperature, Air velocity

ARTICLE INFO

Received 24 Jun 2018

Accepted 4 September 2018

DOI: 10.xxxxx

ISSN: -

AL-MUHANDIS Journal (JMISE)

© 2018 Iraqi Society of Engineers (ISE)

E-mail: jmise@ise-iq.org

Online: www.jmise.ise-iq.org

Office Address: Iraq, Baghdad, Al-Nidhal Q., 103-30-5

CORRESPONDING AUTHOR

Name: Ahmed Jawad Khaleel

Email: ahmed1982_jk@yahoo.com

Research Field: Air-Conditioning

Google Scholar:

1. INTRODUCTION :

Indoor environment affects not on the occupants comfort only, but also on their health and productivity .Most people spend no less than 90% of their times indoor [1]. Indoor environment quality (IEQ) involves several factors (thermal environment, air quality, acoustics and lighting,). Recent studies have proved that an investment in improved (IEQ) is very cost-effective [2-4]. In offices all these factors have an impact on persons; the two most significant factors are thermal environment and air quality [5].

Generally, air flow pattern and temperature distribution within any space play a significant role in determining the quality of the indoor environment and therefore the amount of energy required to condition the air for the space.

There are many international and local standards described recommendations to achieve good indoor environment [6]. Recommended values for the average of air velocity, air temperature, relative humidity, vertical temperature gradient both for winter and summer conditions are listed in these documents. Previous studies showed the arrangement of the air conditioning units has an important effect on the thermal comfort level of the personal space inside test room specially customized for experimental work.

A simulated office room in Denmark equipped with many different personalized ventilation systems showed that such systems have improved the air quality and the subjects evaluated the internal thermal environment as acceptable [7]. Also, In Thailand a study was conducted to evaluate the effect of local air movement (small fans) in a semi controlled environment operating with air-conditioning. The thermal environment was considered highly acceptable by occupants with air temperatures of up to 28°C, with air velocities ranged between 0.5-2.0 m/s [8]. Another study in Japan (chairs equipped with fans) [9]. Showed that the personalized conditioning systems (in regard to thermal comfort) were considered equal or even better than conventional cooling systems [10-13]. Use both of floor fans [14] and the chair equipped with fans [15] made them capable to maintain acceptable thermal comfort conditions with air temperatures up to 30°C. The comfort level inside a test room was studied by using CFD. Air speed was set to 0.1-0.3 m / s while air temperature was set to 22-27 C. The results showed that there exists a considerable

muggy region when using a single traditional air conditioning except near the middle and close to doors [1]. In another study the effect of spot cooling on human thermal comfort was investigated. Two tests were performed, in the first one five conditions combined supply air temperature and volume flow rate while, in the second test, two types of air diffuser were developed. In the work, seven males were exposed for 90 minutes to conditions with and without spot cooling. Also in another important study the results of thermogram showed that spot cooling system without diffusers cooled down only the upper body of subjects, where they felt the draft. On the other hand, it was possible to cool down their whole body using the diffuser. Feeling "thermally neutral. [16]. An Experimental study was performed by developing a localized air-conditioning system (or spot) by providing an air vent and outlet. The desired temperature has been obtained in a specified area using localized air-conditioning system, while higher temperature was measured in other zones [17]. Also it can be showed in other investigations that a localized air-conditioning system was able to provide sufficient thermal comfort for an occupant with lower energy consumption [18].And it achieved 30% to 50% less air flow compared to conventional HVAC under ideal conditions for nozzle location and air flow delivery [19]. The air-conditioning system creates thermally comfortable environment by controlling air temperature, humidity, and indoor air quality. However, the energy consumption in the air-conditioning unit tends to significantly affect economy. Therefore, the reduction in the energy consumption of the air-conditioning unit has become a major concern in many countries. Many efforts have been made to cope with this issue in various ways [20].

Thus one of the effective methods to improve both of thermal comfort for the occupants as well as the power consumption is to use a spot cooling system. In the spot cooling approach, airflow is delivered in a distributed manner by going to distributed air flow delivery much higher air velocities are achieved around the occupants. [19].

In large spaces such as factories or offices rooms, which contain a limited number of persons it is not feasible to control the air in the entire area with HVAC system without massive energy consumption (about 40% of total buildings energy consumption). The air-conditioning in large space targets only the occupied zone and it is important that the occupied zone air-

conditioning satisfies a comfortable feeling of the human body, and decreases the air-conditioning load as much as possible. Therefore, this research attempts to investigate by how much the indoor climate conditions be improved using personalized conditioning through controlling on temperature and velocity of air that will translate to energy savings.

2. EXPERIMENTAL WORK:

An office room with dimensions (L4.8 m × W3.8 m × H3.8m) was used to conduct the designed experiments as shown in Fig. 1. The thermal load of this room was about 7 kW. An appropriate personal space was chosen to study the impact of spot cooling system on thermal comfort of one person (sitting or standing) in this space. Six conduits were implemented to condition the suggested zone, with 40 mm diameter, fixed in different locations using the structure as shown in Fig.2. The considered zone was prepared to accomplish human comfort in a (1m×1m×1.8m) space dimensions. Two spot cooling system cases were tested. In the case-1, two of the six air supply sources were placed overhead at a height of 180 cm from the ground and separated by 37 cm from each other. The other four sources were placed horizontally at levels of 109 cm and 63 cm from the ground as shown in Fig. 3. Air temperature ranged from 13.5 to 15.7°C, and jet velocity between 1.2 to 2.4 m/s were supplied.

been placed horizontally similar to first case, as shown in Fig. 4.



Figure 2. Spot cooling system.

The supply air temperature ranged from 13.3 to 16 °C, and the exit air velocity from 1.2 to 1.8 m/s. Table .1 summarizes the conditions that are used in each case. For both experiments, the initial temperature was 34 °C.

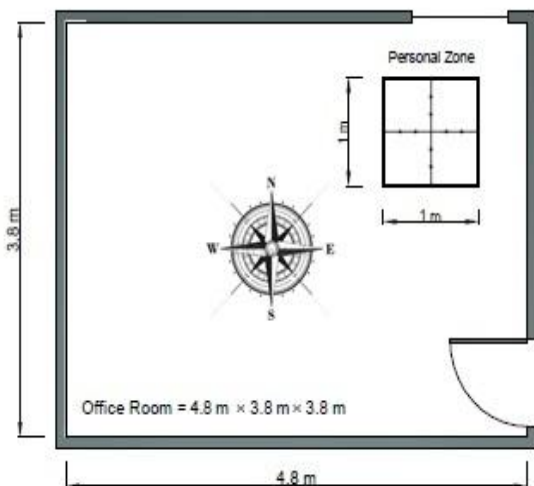


Figure 1. Office test room.

In the case-2 the first two sources were placed at 155 cm height horizontal plane, the other four sources had

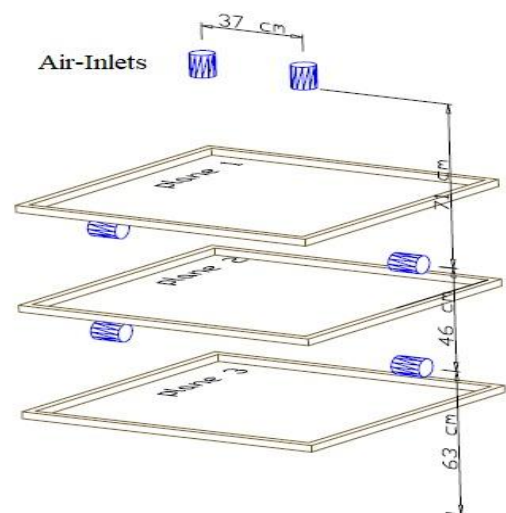


Figure 3. Air Supply distribution for case-1.

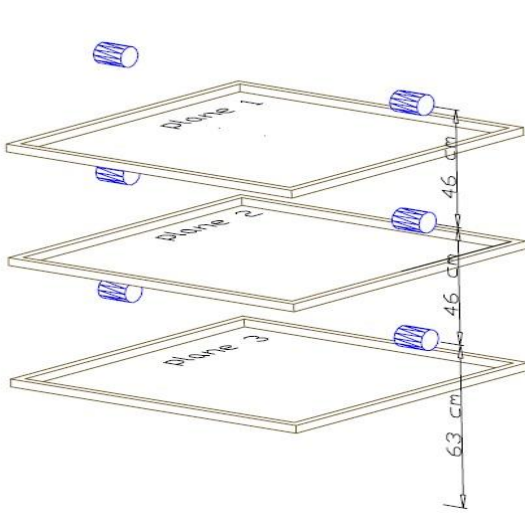


Figure 4. Air Supply Distribution for Case-2.

Twelve thermocouples have been fixed in each one of three planes inside proposed zone (personal zone) to measure the temperature (one reading for every 5 minutes during 30 minute test period) as shown in Fig.5. The Air velocity has been measured in all inlets by using digital anemometer.

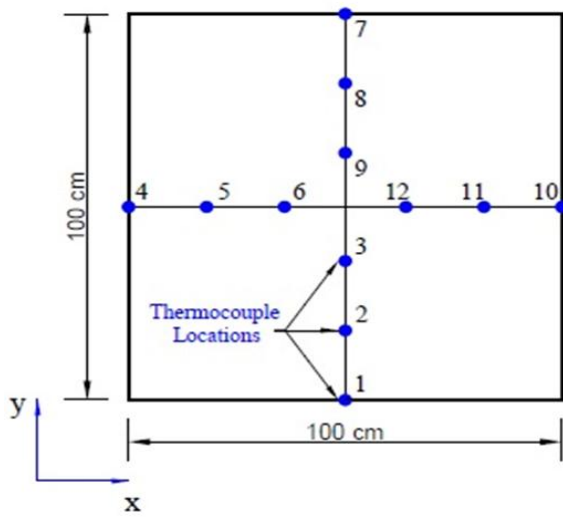


Figure 5. Thermocouple distribution in one level.

Figure.6 shows all cases in vertical and horizontal planes .The planes 1, 2, 3 are parallel to the x-y while the vertical plane shown in this figure is parallel to the x-z .A 18 thermocouples are distributed in this section to measure the air temperature as shown in Figure.7.

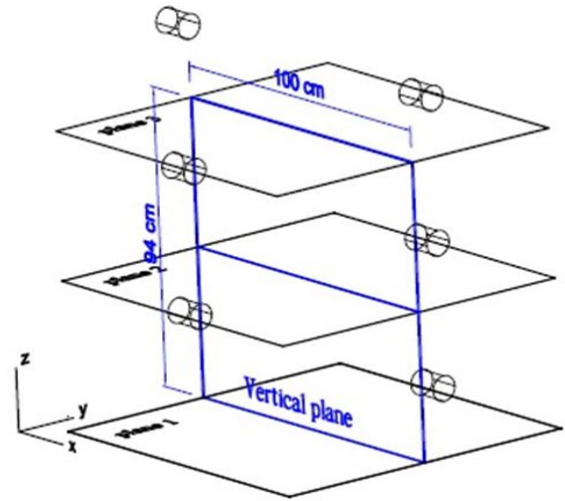


Figure 6. Vertical and Horizontal planes.

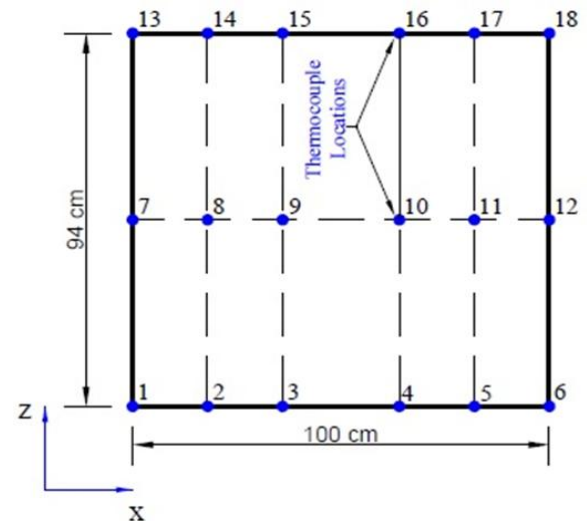


Figure 7. Thermocouple distribution in vertical plane.

Table 1. Summarizes conditions for first and second cases.

	Case-1					
Outlet No.	1	2	3	4	5	6
Supply air temperature[°C]	14	13.8	13.5	15.2	15.7	14.5
Supply air velocity [m/s]	2.3	2.4	1.2	1.3	1.7	1.5
	Case-2					
Outlet No.	1	2	3	4	5	6
Supply air Temperature[°C]	13.3	14.5	14.6	14.5	16	15.2
Supply air velocity [m/s]	1.8	1.7	1.2	1.3	1.7	1.3

3. RESULTS AND DISCUSSION

The following figures present the experimental results of the two cases after 30 min. of air conditioning unit operation.

Figures (8, 9 and 10) show the velocity contours of case-1. In figure (8) the air velocity in plane (1) ranged from (0.02 - 0.3) m/s. while the air velocity in planes (2) was 0.05 m/s in some locations and 0.24 m/s in other locations and (0.04- 0.3 m/s) in plane(3) as show in Figure (9,10) . All these values are increase or decrease according to the position from the air jets. The center of plane exposed directly to the air jets for this reason the air velocity in this place was higher than other regions .Also, the temperature distribution in this region are highly influenced .

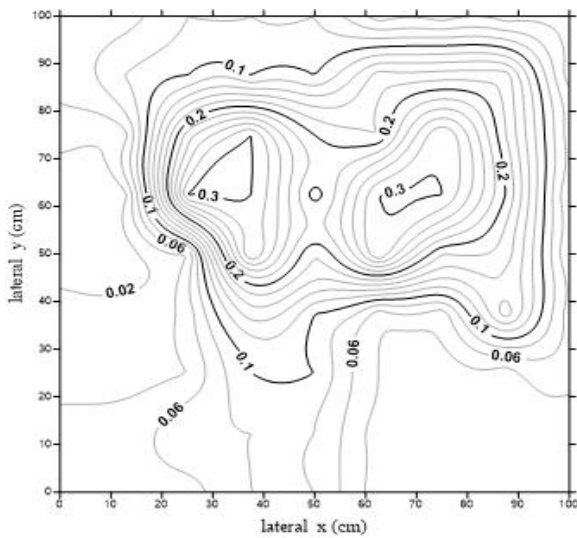


Figure 8. Velocity magnitude Contour (m/s) Case (1) - plane (1)

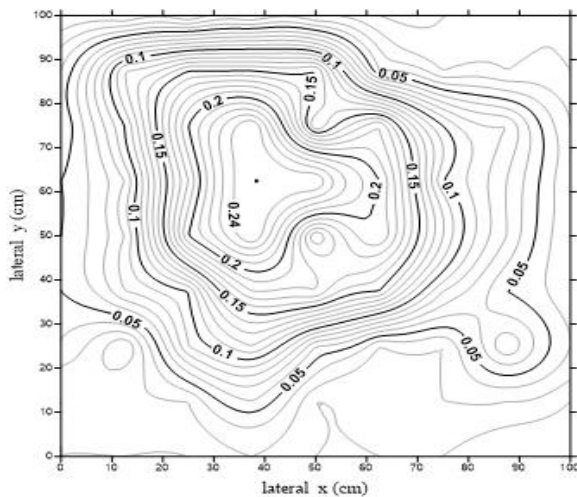


Figure 9. Velocity magnitude Contour (m/s)Case (1) - plane (2)

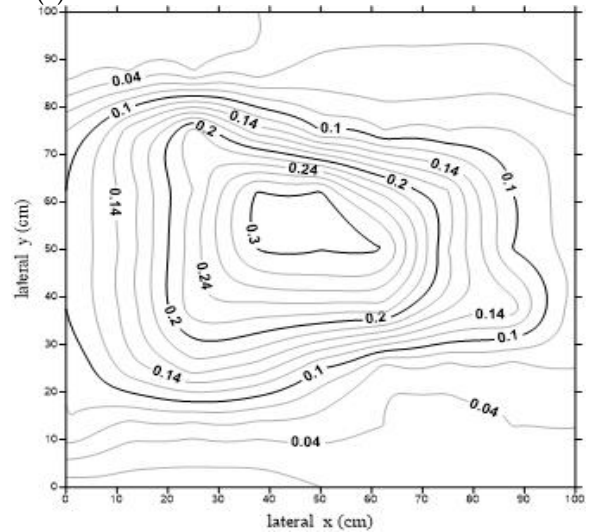


Figure 10. Velocity magnitude Contour (m/s) Case (1) - plane (3)

The temperature distributions for case-1 are shown in figures (11, 12, and 13). Air temperatures in these planes ranged from about (25 °C to 28 °C). Air temperatures decrease when approaching the center of plane (because the effect of overhead and horizontal air jets directed towards the center) and increase gradually to reach 28 °C at the boundaries of planes.

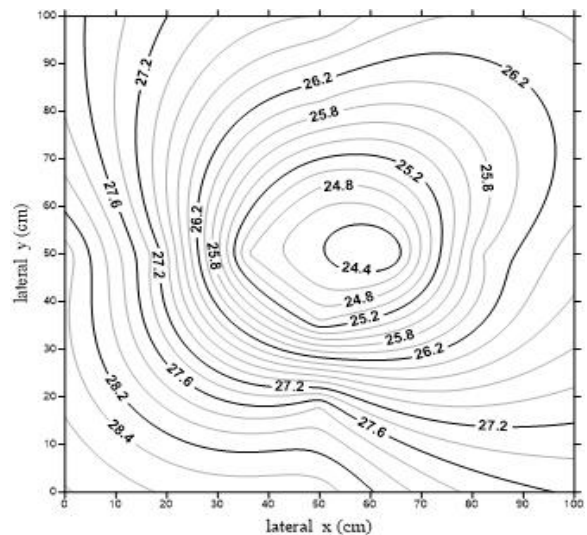


Figure 11. Air temperatures distribution Contour (°C) Case (1) - plane (1)

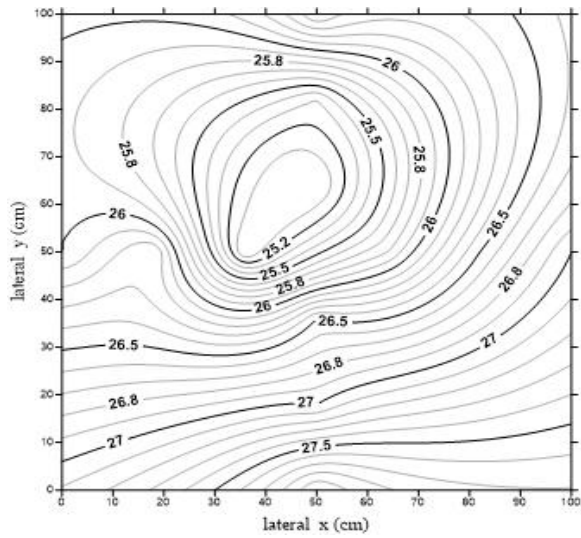


Figure 12. Air temperatures distribution Contour (°C) Case (1) - plane (2).

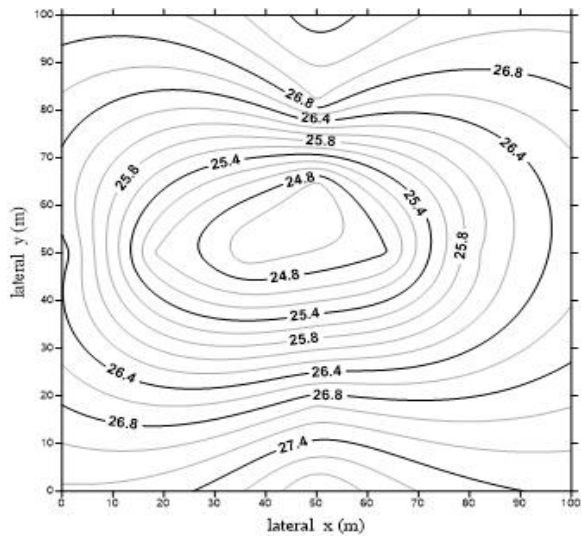


Figure 13. Air temperatures distribution Contour (°C) Case (1) - plane (3).

A suitable thermal comfort was observed inside the zone as depicted from velocity and temperature contours for the case-1.

Figures (14, 15 and 16) show the air velocity for case-2. In plane (1) the air velocity increases gradually from 0.09 m/s at the boundaries up to a maximum value of 0.3m/s at the center of plane. Figures (15 and 16) present contours of velocity in plane2 and plane3 respectively.

Air velocity in these planes ranged from 0.07m/s to 0.3m/s.

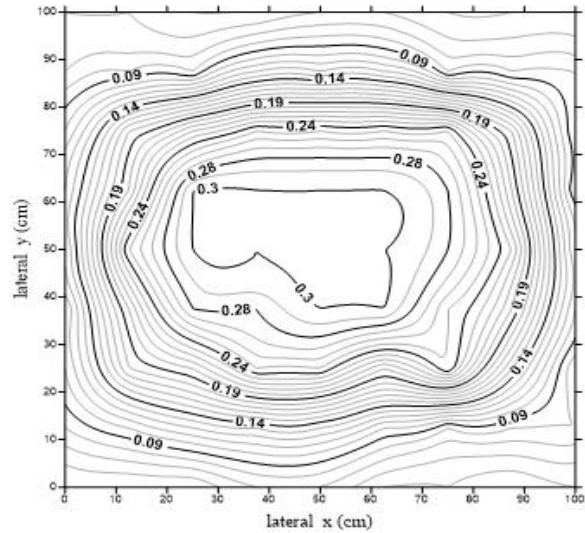


Figure 14. Velocity magnitude Contour (m/s) Case (2) - plane (1).

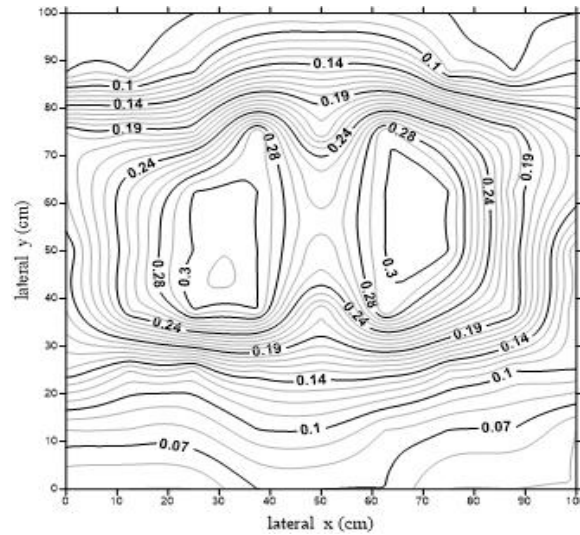


Figure 15. Velocity magnitude Contour (m/s) Case (2) - plane (2).

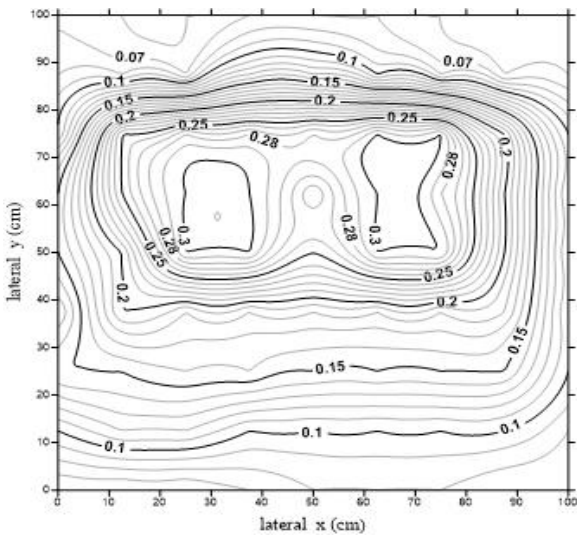


Figure 16. Velocity magnitude Contour (m/s) Case (2) - plane (3).

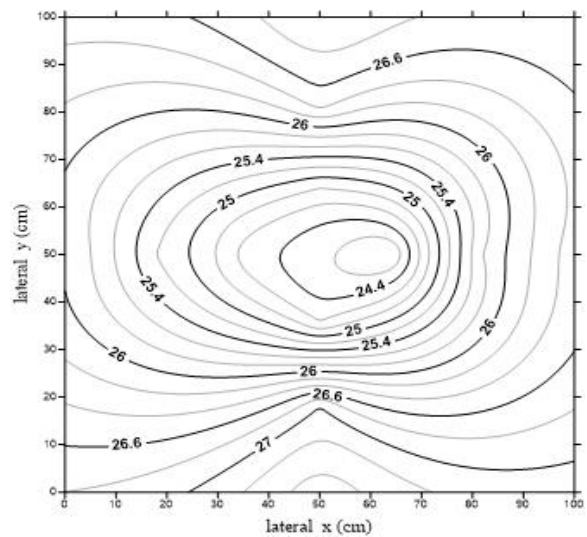


Figure 18. Air temperatures distribution Contour (°C) Case (2) - plane (2).

Figures (17, 18 and 19) represent the temperatures distribution in planes (1,2and3) for the case-2. Air temperatures in plane (1) was about 27°C near the boundaries of planes and decrease markedly to about 25°C at the center. In figures (18 and 19) the air temperatures ranged from 24°C to 27 °C in plane 2 and from 24°C to about 26.8°C in plane3.

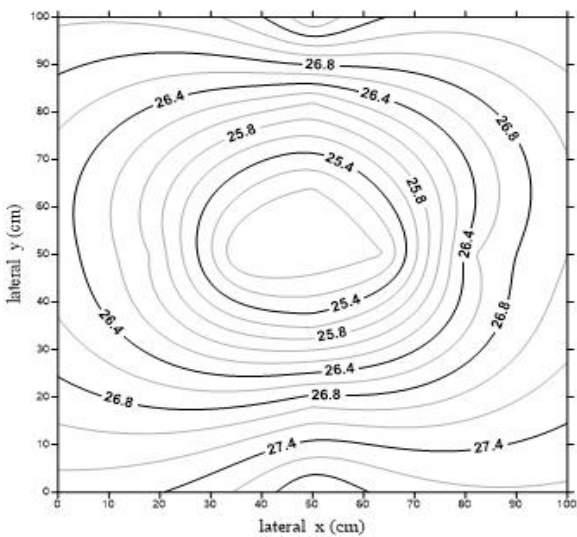


Figure 17. Air temperatures distribution Contour (°C) Case (2) - plane (1).

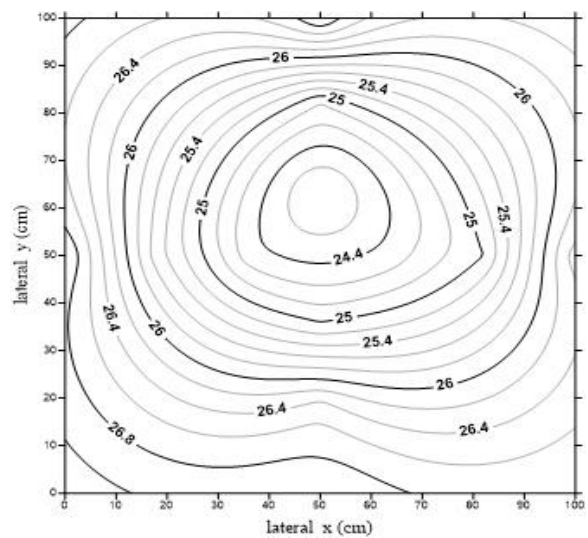


Figure 19. Air temperatures distribution Contour (°C) Case (2) - plane (3).

Figures. (20 and 21) represent the air temperatures distribution in a vertical plane for case-1 and case-2 respectively. In case-1 it can be observed that the temperature decline in region near to or facing the air jets reach about 24.5 °C and 25 °C. Then, it increase gradually whenever it move away from the source of

supplied air to reach more than 27 °C . Also, in the case-2 the temperatures increases and decreases depending on position from the air jet this was because that the velocity of supplied air was low, so it will have a small effect in distant places.

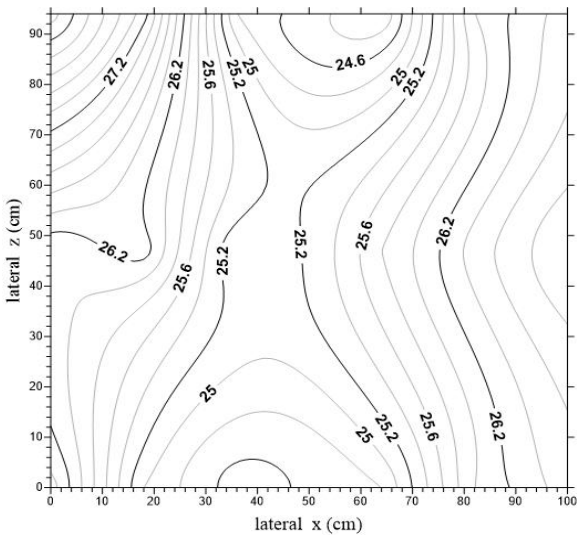


Figure 20. Air temperatures distribution Contour (°C) Case (1) -Vertical plane

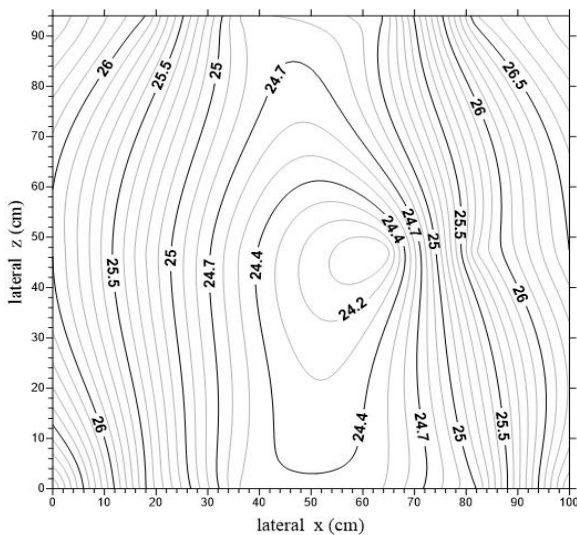


Figure 21. Air temperatures distribution Contour (°C) Case (2) -Vertical plane

Both the case-1 and case-2 provide Appropriate environmental conditions for human comfort, however the case-2 appeared to be more efficient than case-1 in regard to homogeneity of air temperature and velocity due to the present of overhead conduits in case-1 which

affect the velocity distribution and temperature distribution for air within the studied space.

Generally, the air temperatures drop in places near to the air jets and vice versa, that because the low air velocity affect in near places. This effect decreases gradually when its move away from the air source.

Figure (22) shows the temperatures change for 12 nodes in plane 3 -case2 during the starting 30 minutes (one reading in each 5 minutes). The readings were taken using 12 thermocouples fixed in these nodes. The temperature decrease gradually within this time period to reach thermal comfort range for occupants.

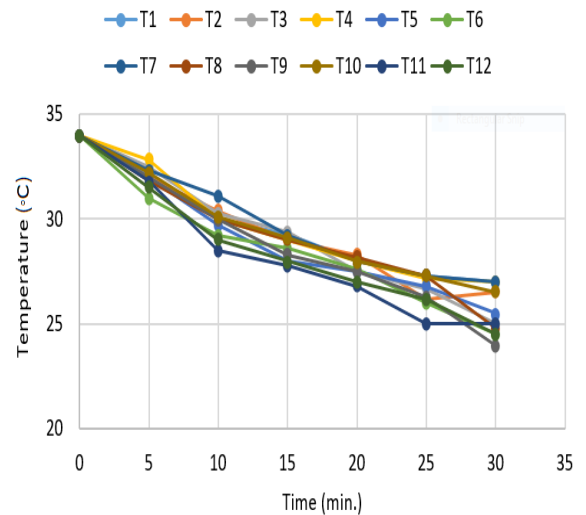


Figure 22. Represents the air temperature with time in case-2

4.CONCLUSION

A spot cooling system has the ability to provide a suitable thermal environment and enhance indoor air quality for occupant .In addition, it is considered as one of the techniques and solutions used to limit of energy problems rather than using traditional cooling methods .Therefore the experimental study has been conducted, to investigate the possibility of using the proposed ventilation system in this paper to achieve of mentioned requirements during 30 minute. The following results can be drawn from this work:

1. The thermal comfort can be created inside personal zone within 30 minutes starting from initial condition.
2. Air velocity produced in the case-2 is more homogeneity throughout the targeted zone than the case-1, then more homogeneity temperature distribution.
3. The second case produced more acceptable variation in temperature with the high (there is a slight and acceptable increase in temperature with increase the high)
4. After 30 minutes, the temperatures were within the acceptable range to provide a suitable thermal environment around the occupant. In the case-1, the temperatures in all measured points ranged from 24.5 °C to 28.5 °C, While In the case-2, its value ranged from 24 °C -27 °C.
5. In the case-1 and case-2 the air velocity in the personal zone ranged from 0.05m/s at the sides of planes to the highest value for it about 0.3m/s at points close to the center due to its locations in front of air sources.

It can be said that the case-2 provide all the possible requirements to supply the comfort conditions around the occupants that because its results were more stable and more acceptable compared to case-1.

5. REFERENCES

- [1] J. Lee, W. Yu "study of indoor temperature and comfort index effect by air -conditioning system" Asia Pacific Conference on Environmental Science and Technology (2012).
- [2] W. Fisk, O. Seppanen, "Providing better indoor environment quality brings economic benefits", Proceedings of Clima, 2007. WellBeing Indoors.
- [3] P. Wargocki, P. Wyon, "Research report on effects of HVAC on student performance", ASHRAE Journal, vol. 48, pp. 22-28, 2006.
- [4] V. Hongisto, "A model predicting the effect of speech of varying intelligibility on work performance", Indoor Air, vol. 15, pp. 458-468, 2005.
- [5] BOMA, What Tenants Want: Building Features, Amenities and Services, Building Owners and Managers Association and Urban Land Institute, USA, 1999.
- [6] R. Kosonen, P.Saarinen, H. Koskela and A. Hole. "Impact of heat load location and strength on air flow pattern with a passive chilled beam system" Energy and Buildings, vol.42, pp. 34-42, 2010.
- [7] J. Kaczmarczyk, A. Melikov, Z. Bolashikov, L. Nikolaev, P.O. " Fanger, Human response to five designs of personalized ventilation" HVAC and R Research, vol.12,pp. 367-384,2006.
- [8] S. Atthajariyakul, C. Lertsatittanakorn, "Small fan assisted air conditioner for thermal comfort and energy saving in Thailand" Energy Conversion and Management,vol.49,pp 2499-2504, 2008.
- [9] S. Watanabe, T. Shimomura, H. Miyazaki, "Thermal evaluation of a chair with fans as an individually controlled system" Building and Environment, vol. 44,pp. 1392-1398, 2009.
- [10] H. Amai, S. Tanabe, T. Akimoto, T. Genma, "Thermal sensation and comfort with different task conditioning systems" Building and Environment, vol. 42 ,pp.3955-3964, 2007.
- [11] J. Kaczmarczyk, A. Melikov, D. Sliva, "Effect of warm air supplied facially on occupants comfort", Building and Environment, vol. 45, pp. 848-855, 2010.
- [12] A. Makhoul, K. Ghali, N. Ghaddar, "Thermal comfort and energy performance of a low-mixing ceiling mounted personalized ventilator system", Building and Environment, vol. 60, pp. 126-136. 2013.
- [13] F. Kalmár, T. Kalmár, "Alternative personalized ventilation", Energy and Buildings, vol. 65, pp.37-44, 2013

- [14] Y. Zhai, H. Zhang, Y. Zhang, W. Pasut, E. Arens, Q. Meng, "Comfort under personally controlled air movement in warm and humid environments", *Building and Environment*, vol. 65, pp. 109-117, 2013.
- [15] S. Watanabe, T. Shimomura, H. Miyazaki, "Thermal evaluation of a chair with fans as an individually controlled system", *Building and Environment*, vol. 44, pp. 1392-1398, 2009.
- [16] H. Ohashi, H. Tsutsumi, S. Tanabe, K. Kimura, H. Murakami, K. Kiyohara, "Subjective Thermal Comfort in the Environment with Spot Cooling System" *Proceedings of Clima 2007 WellBeing Indoors*.
- [17] K. David, S. Chung, T. Ming, W. Ding, "Air-conditioning system of an intelligent vehicle-cabin" *Applied Energy*, Volume 83, Issue 6, pp. 545-557, June 2006.
- [18] S. Kaushik, K. Chen, T. Han, B. Khalighi, "Micro-cooling/heating strategy for energy efficient HVAC System" *SAE Int J Mater Manuf*, vol.4, pp853-63, 2011.
- [19] D. Ghosh, M. Wang, E. Wolfe, K. Chen, S. Kaushik, T. Han, "Energy efficient HVAC system with spot cooling in an automobile-design and CFD analysis" *SAE Int J Passeng Cars - Mech Syst*, vol.5, Issue 2, pp.885-903, 2012.
- [20] A. Manzela, S. Hanriot, L. Gómez, J. Sodré "Using engine exhaust gas as energy source for an absorption refrigeration system", *Applied Energy*, Vol. 87, Issue 4, pp. 1141-1148, April 2010.

Applying a quality improvement program in local industry

Tariq M. Ali¹

¹Department of Applied Sciences, University of Technology

ABSTRACT

Statistical process control field deals with the process that minimizing or eliminating the variation in it until the process reach to the state of statistical control (i.e. only the assignable causes present in the process). There are seven tools to get this target, this work considered these tools, and three of them applied in an industry, General Pipe Company. These tools are: histogram, flow diagram, and check sheet. The importance of the application of these tools lies in the control and verification about the properties of the pipes to the specifications of the company, these properties includes hydraulic pressure test, compression testing, creep rupture strength, physical properties tests such as length, diameter and thickness, testing the roughness of the internal surface of the pipes, and crack resistance test. Procedures and results of this study are demonstrated separately, and drew some conclusions about applying the quality improvement program. One of the main results of this study is that there is a real failure in implementing the quality control programs, where there is a deviation in the average production process in terms of the diameter of the pipes and the process capability is somewhat low, due to the presence a percentage of defectives due to the large dispersion in the production process.

KEYWORDS

histogram, variation, process, quality, improvement

NOMENCLATURES

C_p Process capability
L.S.L Lower specification limit
U.S.L Upper specification limit
 σ Process standard deviation

ARTICLE INFO

Received 18 September 2018

Accepted 27 November 2018

DOI: 10.xxxxx

ISSN: 2413-0230

AL-MUHANDIS Journal (JMISE)

© 2018 Iraqi Society of Engineers (ISE)

E-mail: jmise@ise-iq.org

Online: www.jmise.ise-iq.org

Office Address: Iraq, Baghdad, Al-Nidhal Q., 103-30-5

CORRESPONDING AUTHOR

Name: Tariq M. Ali

Email: tarekza2001@yahoo.com

Research Field: Industrial Engineering

Google Scholar: scholar.google.com/citations?user=OTb5Fj0AAAAJ&hl=ar

INTRODUCTION

The concept of quality improvement was formalized by P. B. Crosby at the Martin Company in the USA in 1961 and has been further developed by many companies since then.' As used in ITT (International Telephone & Telegraph) , the quality-improvement program is a 14-step procedure for defect prevention and summarized in a short booklet entitled Quality Improvement through Defect Prevention, of course, many variations of the program are possible and many of its elements reflect long-established quality control principles, but the need for an overall planned program is inescapable and, in practice, although there have been many attempts, it has not proved possible to devise effective procedures that have departed seriously from the steps given in the quality-improvement booklet. [1]

Although originated in the USA, the program has now been applied with striking success in many European countries. In the UK one unit was receiving serious complaints about product conformance from its major customer. By applying the program, for nine major product lines the percentage defective as recorded by the customer was reduced by a factor of 4. At the same time the ratio of testers and inspectors to direct operatives was reduced by 21 percent.

In Germany another unit reduced its quality-cost to sales ratio in 1968 to 864 per cent of the 1967 value and in 1969 to 802 per cent, thereby saving DIM 34 million. Various measures of level of conformance improved simultaneously: tool-making defects were reduced from 40 per cent to 1.2 percent; defective piece parts were reduced from 32 percent to 0.4 percent; electronic assembly defects on printed circuit boards were reduced to one-eighth and so on. During six months the average number of defects made by each worker was reduced from forty per month to ten per month. In Italy a company reduced its quality-cost to sales ratio from 90 per cent in 1968 to 75 percent in 1969 and 74 percent in 1970; In Belgium another company reduced the ratio from 88 per cent in 1969 to 75 percent in 1970, saving BF 95 million. Both these companies improved their level of product conformance simultaneously. Other examples could be given involving companies in Spain, Portugal and France. In all cases quality costs were reduced but with no sacrifice of quality-in fact there was an improvement in the level of product conformance. [1]

1. MANAGEMENT COMMITMENT

The fourteen steps of the quality improvement program are summarized in Fig. 1 which also may give a time table for their application extending over one year or more. [2]

The first step is "management commitment" Without an active commitment by the general manager of the unit and full support by his entire department heads, the major benefits of the program cannot be achieved. In the entire successful program described above the complete support of the unit general manager was a common feature.

In addition to the commitment of active support for the whole quality-improvement program, the general manager at the start of the program should formally state the quality policy of the unit and publicize it so that everyone in the unit is completely familiar with it. The ITT ((International Telephone & Telegraph) quality-improvement booklet lists five things that the quality policy should not be: [3]

1. It should not be a treatise on the 'Economics of Quality'. There is no such thing as an Economical Level of Quality and it is always cheaper to do the job properly. There are economic levels of inspection, test laboratory equipment, secretaries, food servings and other functions, but there is no "Economic Level of Quality".
2. The Quality Policy should not have a number in it. Stating allowable nonconformance is no way to get what you want because no one notices the number for what it is. They just know it is there and allow for it."
3. It should not indicate any method of deviating from the policy. If it does immediately there will be a procedure written on that method and meetings will be held to train people extensively in the procedure to the reduction of the original intent."
4. It should not delegate the responsibility for evaluating performance to the policy. This must be the prerogative of the Chief Executive even though he will have others gather the information for him.
5. The policy should not be hidden in a book reserved for executive personnel only. It should be stated, re-stated and publicized until everyone knows, understands and believes it.

Step	Action	Purpose
Step 1	Management commitment	To clarify where administration remains on quality
Step 2	The quality improvement team	To start the quality development program
Step 3	Quality measurement	To give a show of present and potential nonconformance problems in a way that licenses target assessment and remedial activity
Step 4	The cost of quality	To characterize the elements of the quality cost, and clarify its utilization as an administration device
Step 5	Quality awareness	To give a technique for raising the individual concern felt by all work force in the organization toward the conformance of the product or benefit, and the quality notoriety of the organization
Step 6	Corrective action	To give a precise technique for settling the problems that are distinguished through past activity steps
Step 7	Zero defect planning	Study the various activities that must be undertaken in preparation for launching the zero defects program officially
Step 8	Supervisor training	To characterize the sort of preparing that administrators require keeping in mind the end goal to effectively complete their part of the quality improvement program
Step 9	Zero defects day	To make an occasion that will give all employees a chance to acknowledge through an individual ordeal that there has been a change
Step 10	Goal setting	To transform vows and duties without hesitation by urging people to set up change objectives for themselves and their gatherings
Step 11	Error-Cause removal	To give the individual worker a technique for imparting to administration the circumstance that make it troublesome for the representatives to meet the promise to progress
Step 12	Recognition	To welcome the individuals who take an interest
Step 13	Quality Councils	To unite the expert quality individuals people for planned communication on a regular basis
Step 14	Do it over again	To accentuate that the quality improvement program never closes

Figure 1. Fourteen steps for quality improvement program [2]

2. STATISTICAL PROCESS CONTROL

Statistical Process control (SPC) charts use sub-grouped data. The obligation regarding quality in any process must lie with the administrators of that process. To satisfy this obligation, individuals must be supplied with the instruments important to: [4]

- Know whether the process is capable of meeting the requirements.

- Know whether the process is meeting the requirements at any point in time.

- Make correct adjustments to the process or its inputs when it is not meeting the requirements.

The strategies of statistical process control (SPC) will enormously aid these stages. To start to check and dissect any process, it is important first to recognize what the process is and what the sources of inputs and outputs are.

Many processes are effectively comprehended and identify with known techniques e.g... Drilling a hole, compressing tables filling cans with paint polymerizing chemical using catalysts. Others are less effortlessly identifiable, e.g. servicing a customer, delivering a lecture, storing a product in a warehouse, in putting to a computer.

3. THE MAGNIFICENT SEVEN

In quality control and quality assurance some methods have proved so beneficial over the years that they are used constantly in top companies. Some of graphical methods are so widely utilized by almost every level of the company that they have nicknamed the magnificent seven. These simple tools should be understood and routinely used by everyone they are: [3]

- 1) Control charts
- 2) Check sheets
- 3) Histograms
- 4) Pareto diagrams
- 5) Ishikawa diagrams
- 6) Scatter plots
- 7) Flow charts

3.1 Check sheet

One of the simplest yet most effective graphical methods is the check sheet: A check sheet is an easy way to collect data, analyze the data at a glance and present the results. This is often enough to get the required action see Fig.2

Type of error	Count	Score
Reversed letters		5
Missing letters		8
Extra letters		5
Wrong letters		10
Total errors:		28

Figure 2. Check sheet [3]

The purpose of a cheek sheet is to classify, stratify, and tally observed data in the form of occurrences of events or out comes so that we can obtain a feel for relative frequency and dispersion of the events or out comes.

3.2 Histogram

It describes the variation in the process as illustrated by Fig.3 this histogram graphically shows the process capability and, if desired the relationship to the specifications and the nominal. It also suggests the shape of the population and indicates if there are any gaps in the data.

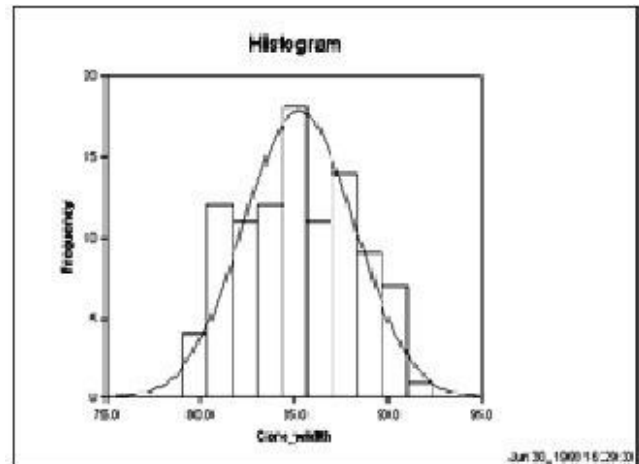


Figure 3. Typical histogram [3]

3.3 Flow diagram

For many products and services, it may be useful to construct a flow diagram. It is schematic diagram that shows the flow of the product or service as it moves through the various processing stations or operation. The diagram makes it easy to visualize the entire system, identify potential trouble spots, and locate control activities.

The diagram shows who is the next customer in the process, thereby increasing the understanding of the process.

Flow diagrams are best construct by a team, because it is rare for one individual to understand the entire process.

Improvements to the process can be accomplished by eliminating steps, combining steps, or making frequently occurring steps more efficient.

4. PROBLEM SOLVING METHOD

The project team achieves the optimal results when it operates within the framework of the problem - solving method.

In the initial stages of process - improvement program, quick results are often obtained because the solutions are obvious or someone has a brilliant idea. However, in the long term, a systematic approach will yield the greatest to process improvement has seven phases (4):

1. Identify the opportunity
2. Define the scope

3. Analyze the process
4. Develop the optimal solutions
5. Implement and study results
6. Standardize the solution
7. Plan for the future

In fact, some techniques such as the control chart can be effectively utilized in more than one step. Process improvement is the goal, and the problem – solving process is a framework to achieve that goal.

5. EXPERIMENTAL WORK

This study deals with the procedures that are followed during applying the quality improvement program in GPC (General Pipe Company), three SPC (Statistical Process Control) tools selected for this study due to the time limitation and efforts.

This study will start by explaining the step of process selection and the quality characteristic of the study. These two steps are described in the next two sections.

6. PROCESS SELECTION

The Irrigation Pipes Department consists of two production lines, one is used to produce pipes, and the other is used to produce joints.

Unfortunately product of this department is not subjected to any quality tests, because the use of the pipes to transfer the water in the farms, make the quality sense has no value in the production stages of these pipes.

The third department in the General Pipe Company is producing the longitudinal welded pipes, there are two lines of production, one is used to produce pipes of small diameters, and the other produce large diameter pipes 1 - 4 inch.

Engineers in charge of this department have emphasized the importance of quality control programs in this department, also the production process in this department can be considered as a mass production because each order require at least 75 days of 8 hours shift for 2 shifts per day.

In addition, any variation in some of the product quality characteristics will cause some troubles in the production stage or the using stage of this product, which will affect the product quality.

According to these considerations the process of producing the longitudinal welded pipes is selected for this study.

7. SELECTION OF THE QUALITY CHARACTERISTICS

Any product may have more than one quality characteristic, whether variable or attribute, these characteristics have different effectiveness on the product quality level, but any practical study should be performed, such that critical quality characteristics are selected.

The product on hand has approximately four important quality characteristics, these characteristics are to be demonstrated in order to determine the most critical one to be selected for the purpose of the study. These characteristics are:

7.1 Pipe thickness

Because pipes are subjected to high pressures during the using stage, pipe thickness is considered an important factor for pressure endurance.

The pipe thickness depends on pipe diameter and the liquid flow rate, so as the diameter is increased the pipe thickness has to be increased.

As denoted before, raw materials are received as steel rolls, the thickness is determined according to the pipe diameters needed. Because of the strip thickness is not affected during the manufacturing process, so the initial roll thickness test is sufficient to ensure that the pipes have the required thickness.

The responsible engineers said that, "an undesirable variations of the pipe thickness is unexpected thing during the manufacturing process, this is at least from our experience with pipes manufacturing".

7.2 Pipe length

The manufactured pipes have length between 6 to 8 meters depending on the specific orders.

The cutting process starts immediately after the welding process. By automatic cutting saw, where there is a wheel contacting to the pipe surface and works as a sensor for the automatic cutting saw, this wheel is adjusted to send a signal to the automatic cutting saw after certain number of rotations.

The number of rotations is determined according to the length of the pipe produced, after the signal is received, the wheel is reset and starts the counting again.

7.3 Pipe diameter

Pipes are classified according to the pipe diameter. The following Section describes the importance of the pipe diameter, as a quality characteristic that should be maintained at the target level, this information is the result of discussion with engineers in charge at the department.

In fact, pipe diameter starting from the cutting roll stage to the required width, so this operation should

receive some attention, as pipes are formed in the brining group, the two strip edges are heated, then pressed to joint together until final pipe diameter appears.

Using cutting tool to clean the welding area along the pipe will cause some forces acts on the pipe surface, where if any error occurs during the roll or the cutting tool adjustment that will cause an increasing or decreasing in the pipe diameter.

Also, if the tool of the automatic cutting machine is not with sharp edged, the force acting during the cutting will increase and cause a diameter error.

The pipe ends then is subjected to a force caused by the cutting tools of the beveling machine. This force acts on the pipe surface at the same time and the resultant of these forces should be approximately equal zero on the pipe.

If any of the two tools has corroded then one force will act on the pipe and causes a decrease or an increase in the pipe diameter according to the force direction.

The wear of the tool cut will cause failing of the beveling process, where a thin layer will appear at the end of pipe.

After the quick forces and stresses acting on the pipe during the manufacturing process which may cause undesirable variation on pipe diameter, selection of pipe diameter as the quality characteristic for the purpose of this study is due to the following reasons:

- a. Pipes are classified and ordered according to the pipe diameter, where the flow rate mainly depends on the pipe diameter, so if with any change in the pipe diameter the flow rate is changing.
- b. Variation in pipe diameter may reflect an error of the welding process.
- c. Variation of pipe diameter may be considered as an indicator of serious problem in beveling machine, especially the life of the cutting tool.
- d. During the water test , the pipes is gasped by the rubber seal to prevent water leakage from the ends, if any change in the pipe diameter the rubber seal may loss its function which cause error in the machine readings.
- e. The threading machine is adjusted according to the pipe diameter, so any changes in the pipe diameter means changing of the depth of threading, which

may prevent the connection of this pipe with the others.

- f. Forming the thin layer at the end of the pipe means zone with no threading.

For this reason the teeth of threading machine will act on the metal at this area.

8. DATA COLLECTION

In fact there are two types of data required for this study:

- 1) Numerical data: these are the pipe diameter measurement required to construct the histogram,
- 2) Quantitative data: related to the process sequence, flow diagram of the department, and some information about the maintenance program for the machines of the department.

Table 1 represents some statistics of the sample collected, then the histogram in fig.4 shows the distribution of these data for pipes diameter.

Due to the barriers of the time to enlarge the sample, this study dependent on this sample as the population of the process, such that the average of this sample consider to be the average of the process at this time.

The design specification and tolerances of the manufactured pipes follows the British specification BS.1387: 1985 (thickness class B) for welded pipes as illustrated in fig.5.

The two types of data have been collected at the same time, with the help of the engineers in the departments.

Table 1. Sample statistics

Variable	Quality average	Variable	Quality average
Sample Size	55	Average	27.149
Median	27.155	Mode	27.167
Geometric Mean	27.102	Variance	0.0112
Standard Deviation	0.143	Standard error	0.00820
Minimum	26.900	Maximum	27.4125
Range	0.5125		

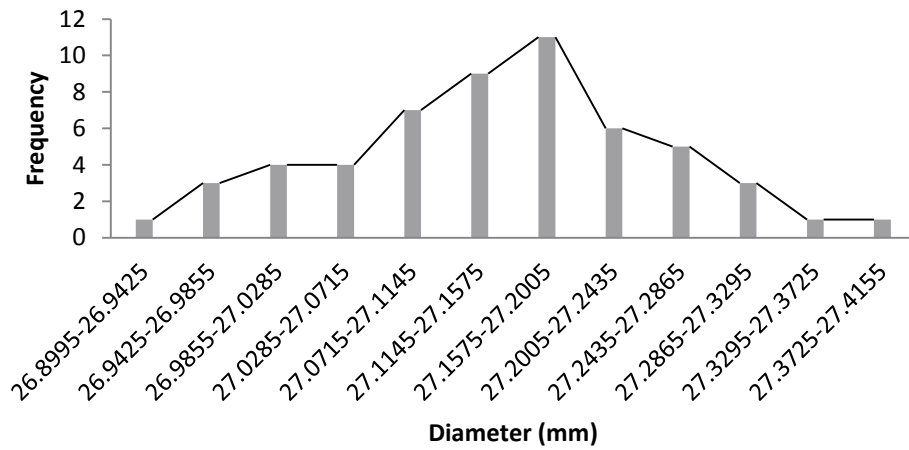
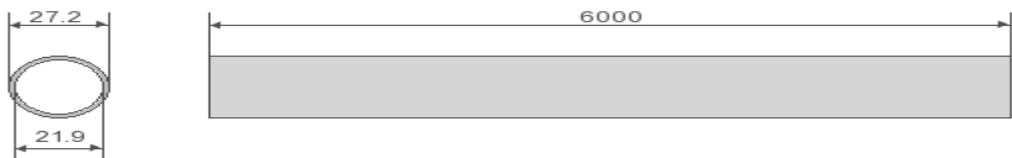


Figure 4. Histogram for pipes diameters

Thickness Class	Nominal Size		Outside Diameter	Wall Thickness	Inside Diameter	Calculated Weight				Test Pressure	
						Plain Ends		Threads & Coupling			
	mm	in	mm	mm	mm	kg/m	kg/6m	kg/m	kg/6m	kgf/cm ²	Psi
Medium "B"	90	3-1/2	101.1	3.65	93.8	8.75	52.50	8.93	53.57	50	700
	100	4	113.9	3.65	106.6	9.89	59.34	10.20	61.20	50	700
	15	1/2	21.7	2.65	16.4	1.22	7.32	1.23	7.38	50	700
	20	3/4	27.2	2.65	21.9	1.58	9.48	1.59	9.54	50	700
	25	1	34.2	3.25	27.7	2.44	14.64	2.46	14.76	50	700
	32	1-1/4	42.9	3.25	36.4	3.14	18.84	3.17	19.02	50	700
	40	1-1/2	48.8	3.25	42.3	3.61	21.66	3.65	21.90	50	700
	50	2	60.8	3.65	53.5	5.10	30.60	5.17	31.02	50	700
	65	2-1/2	76.6	3.65	69.3	6.51	39.06	6.63	39.78	50	700
	80	3	89.5	4.05	81.4	8.47	50.82	8.64	51.84	50	700
	100	4	114.9	4.50	105.9	12.10	72.60	12.4	74.40	50	700
	125	5	140.6	4.85	130.9	16.20	97.20	16.7	100.20	50	700
	150	6	166.1	4.85	156.4	19.20	115.20	19.8	118.80	50	700
	200	8	216.3	5.80	204.7	30.10	180.60	--	--	50	700
250	10	267.4	6.60	254.2	42.40	254.40	--	--	50	700	



Nominal size (DN)	Designation of thread	Outside diameter		Thickness mm	Mass of black tube	
		max. mm	min. mm		Plain end kg/m	Screwed and socketed kg/m
8	1/4	13.9	13.3	2.3	0.641	0.645
10	1/8	17.4	16.8	2.3	0.839	0.845
15	1/2	21.7	21.1	2.6	1.21	1.22
20	1/4	27.2	26.6	2.6	1.56	1.57
25	1	34.2	33.4	3.2	2.41	2.43
32	1 1/4	42.9	42.1	3.2	3.10	3.13
40	1 1/2	48.8	48.0	3.2	3.57	3.61
50	2	60.8	59.8	3.6	5.03	5.10
65	2 1/2	76.6	75.4	3.6	6.43	6.55
80	3	89.5	88.1	4.0	8.37	8.54
100	4	114.9	113.3	4.5	12.2	12.5
125	5	140.6	138.7	5.0	16.6	17.1
150	6	166.1	164.1	5.0	19.7	20.3

NOTE: Maximum and minimum outside diameters meet the requirements of ISO 65

Figure 5. BS.1387: 1985 (thickness class B) for welded pipes

9. PROCESS CAPABILTY

From table 1 , we can see the sample standard deviation(S) equal to 0.143 , so we can estimate the process standard deviation for whole production from this value ($\sigma = 0.143$).

Also, from fig.5 which represented the B.S 1387 for welded pipes, we can see the lower and upper specification limits (L.S.L & U.S.L) for pipes with diameter 27.2 mm class B are 26.6 mm and 27.2 mm respectively , that is mean the nominal value for this specification is 26.9 mm .

To calculate the process capability (C_p) for this type of pipes:

$$C_p = (U.S.L - L.S.L) / 6\sigma \dots\dots\dots (1)$$

$$C_p = (27.2-26.6) / (6 \times 0.143)$$

$$C_p = 0.7$$

10. FLOW CHART

This is one of the most important techniques used in the quality improvement program, where it gives the ability to make overview to the process to see if there any need to cancel or to group any activities which will lead to decreasing the time of the production process or the time of material handling.

This technique also considered where the data have been collected with the help of the engineers in the department. The flow chart of the department is drawn and shown figs.6, 7, and 8.

These figures showed the flow diagrams of the industrial process, these figures subject to the study with the engineers of the department to search about the ability of doing something about the time to produce one pipe, if there is an ability to decrease it by changing or combining or canceling some unnecessary activities in the process.

Finally, we reach to that, the present flow diagram of this process is the most appropriate one in the current time due the highly cost required for any changes.

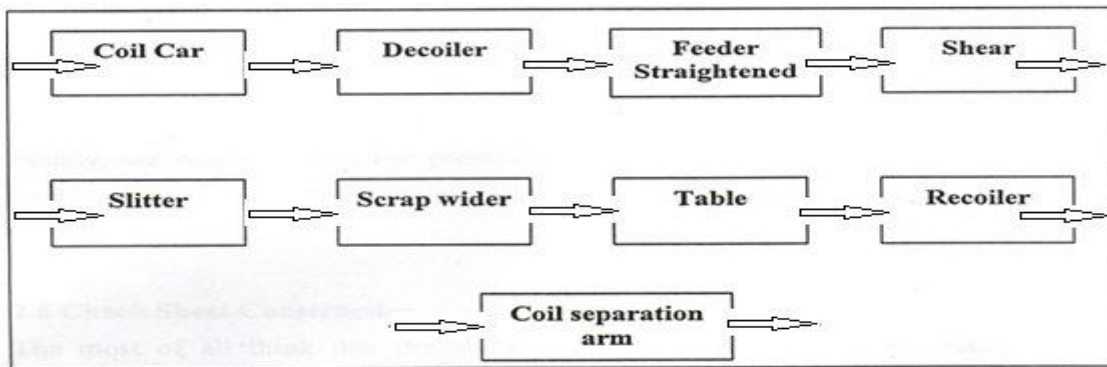


Figure 6. Slitting line for heavy coils

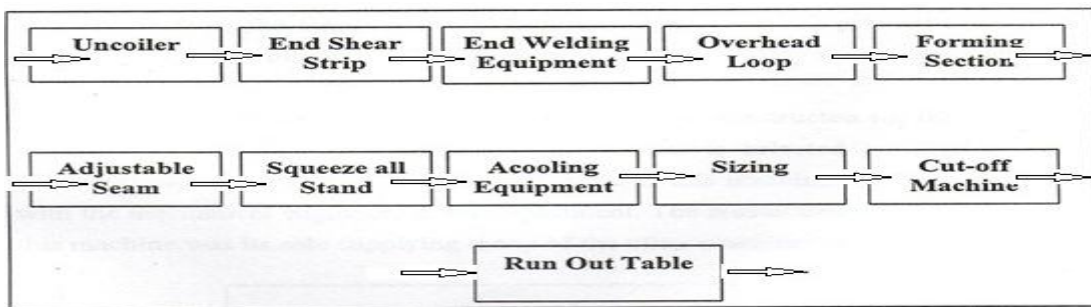


Figure 7. Strip preparation of tube mill

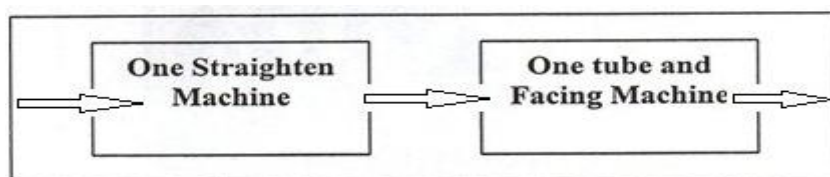


Figure 8. Finishing section

11. CHECK SHEET CONSTRUCTION

The most of all think that the check sheet is a tool used only for the maintenance department, where some time calls it daily check or weekly and so on. It is one of the most common assignable cause effect in the quality of the product and then shifts the process from the target is the machine failures, so if we can prevent this failure before it happened, that is mean we protect our product quality from deterioration.

In this study the check sheet receives attention to be constructed for the industrial process that subject to the study. Only one machine is selected for this purpose, (Compressor) which illustrated in fig, 9. . The reason behind the selection of this machine has been discussed with the mechanical engineers in the company , the reason behind the selection of this machine because it's a main air supplier for most other machines in the company, so any failure in a compressor will effect on other machines.

Eight elements of maintenance should be considered for the machine determined by the discussion with the mechanical engineers, these elements considered for our Check Sheet. Thirteen days of study have been considered for the check sheet, some of these sheets are represented below.

Table 2 shows the typical check sheet constructed for the process and the result are checking represented also. Check sheet of another day represents in table3.

Table 3 shows that, the compressor was failed during this day, so there is no any activity checked in this day.

Table 4 shows that the lamp of activity 1 is on, which mean there is error in the machine, the cell of remarks denote the procedures should be followed to repair the failure.

Table 5 is a check sheet of the 14th day of study, where the sheet shows the lamp of the air filter is on, so the filter should be changed.

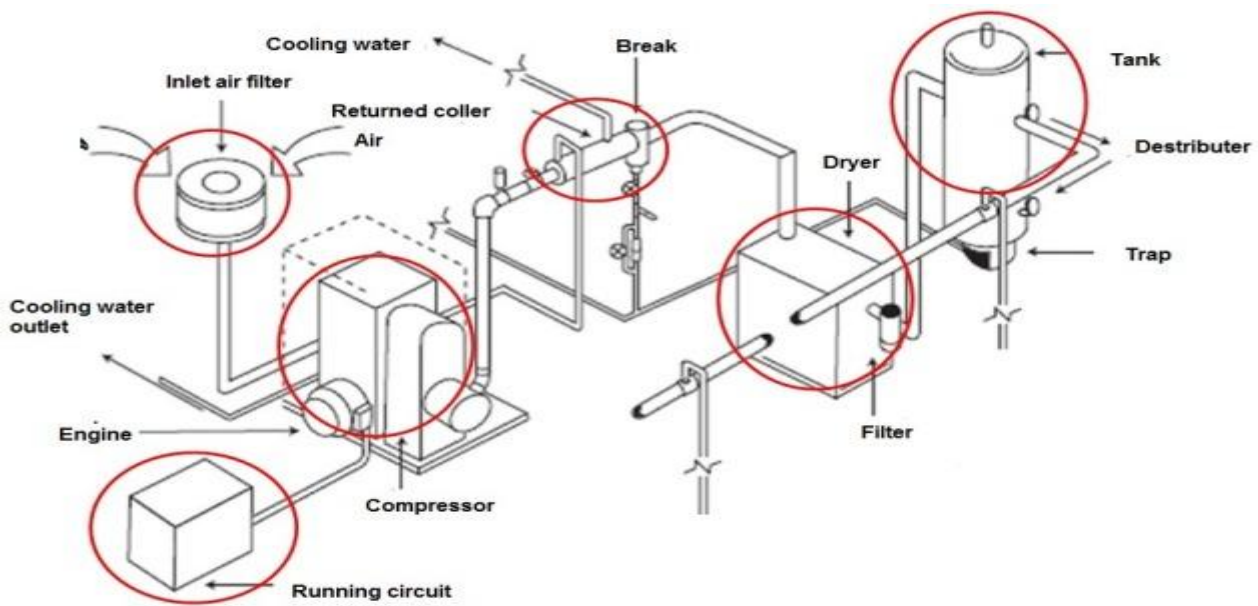


Figure 9. Main compressor

Table 2. Check sheet for the first day of study

No.	Activity	Daily	Weekly	Remarks
1	Check the service of indicator lamp	On		
2	Check the service of air intake filter	Ok		
3	Renew air intake filter	Ok		
4	Check the service of regulating system	Ok		
5	Check oil level	High		
6	Inspection the performance of moisture tap	Ok		
7	Check air discharge temperature	42 C ⁰		
8	Check air / oil temp. Outlet of compressor element	70 C ⁰		

Table 3. Check sheet for the 7th day of study

No.	Activity	Daily	Weekly	Remarks
1	Check the service of indicator lamps			
2	Check the service of air intake filter			
3	Renew air intake filter			
4	Check the service of regulating system			Failure in Fan
5	Check oil level			
6	Inspection the performance of moisture tap			
7	Check air discharge temperature			
8	Check air/oil temp. Outlet of compressor element			

Table 4. Check sheet for the 10th day of study

No.	Activity	Daily	Weekly	Remarks
1	Check the service of indicator lamp	On		Change oil
2	Check the service of air intake filter	Ok		
3	Renew air intake filter	Ok		
4	Check the service of regulating system	Ok		
5	Check oil level	High		
6	Inspection the performance of moisture tap	Ok		
7	Check air discharge temperature	42 C ⁰		
8	Check air / oil temp. Outlet of compressor element	70 C ⁰		

12. RESULTS & DISCUSSION

We can obtain some results from this practical study, as follow:

1. From the numerical data that we obtained for a sample to construct a histogram, the range value was (0.512 mm) for diameters, so it is less than specification tolerances value (0.6mm)
2. The nominal diameter value of specification which used is (26.9 mm) , while the sample average which represent the process mean is (27.149 mm) , so there is a deviation in a production mean about (+0.249 mm).
3. The standard deviation of a sample (S) was about (0.143 mm) , this value can represent the standard deviation for whole production (σ) , this value is more accurate than the sample range as a scale for dispersion , because it takes in account the whole sample not only the maximum and minimum values as a range.
4. This study found that production process capability (C_p) equal to 0.7, so $0.67 < C_p < 1$, we can say the process is not adequate for the job, and a

process analysis is necessary, requires serious modification to reach a satisfactory quality.⁽⁹⁾

5. It is recommended to re-setting the process mean (27.149 mm) and shift it towards a specification nominal value (26.9mm), because most of defective pipes have diameters more than upper specification limit (U.S.L).
6. There is a clear negligence in the maintenance and maintenance of the compressor, which is the main element in the machines of the company, in terms of repeated failure of the compressor fan and lack of good maintenance of filters
7. Find all appropriate solutions to reduce the standard deviation of the production process, to minimize defectives beyond the specifications.

13. CONCLUSION

Some important points can be drawn from this work, these points summarized as conclusion of the present work and listed below:

1. Due to the lack of experience for the quality control meaning in our organizations, these techniques are neglected.
2. Applying the quality control program requires group efforts to plan and achieve it, as the group consist from the organization staff, it would become more easily and vice versa.
3. The value of the process shift has no meaning for the management but if this value changed in the form of money or number of defective items then the management may take steps to correct the problem.
4. The flow diagram not easy to be change that is due to the cost of changing the layout of the company or the sequence of the machine.
5. In case of large process, the flow chart should be divided in to many parts to be easier to see the current situation.
6. Check sheet is the most common tool between the workers of any organization, but some time, it considered as a tool for the maintenance department only.
7. The process that subject to the study has a shift in the average of the pipe diameter.
8. One can extend this work by applying the other SPC tools such as Control Charts, Pareto diagram, or Cause and Effect Analysis.
9. Comparing between the effect of applying the quality improvement program between two organizations or more.

14. REFERENCES

- [1] M. Grocock , The Cost of Quality, Pitman Publishing, London,(1974).
- [2] D.K. Adhwarjee, Exploring Crosby's Fourteen Steps to Quality Improvement Applied to Industry,International Journal of innovative technology and research, Volume No. 1, Issue No. 6, October – November (2013) 544 – 546.
- [3] S. Vestnik , Basic Quality Tools in Continuous Improvement Process, Journal of Mechanical Engineering 55, (2009) 2.
- [4] J.S. Oakland, Oakland on Quality management, 3rd .ed., London, (2004).
- [5] J. Henderson, The Quality Problem Solving Method and its Effectiveness at Nortech Inc, Bemidji stateuniversity, (2009).
- [6] Montgomery C. Douglas, Introduction to StatisticalQuality Control. John Wiley&sons, (1991).
- [7] B. Radej , J. Drnovsek, G. Beges , An overview and evaluation of quality improvement methods fromthe manufacturing and supply chain perspective,Advances in Production Engineering & Management journal, Volume No. 12, Issue No. 4, December (2017) 388–400.
- [8] S. Muhammad, Quality Improvement Of Fan Manufacturing Industry By Using Basic Seven Tools Of Quality: A Case Study, Journal of Engineering Research and Applications, Vol.5, Issue 4, (Part 4), April (2015) 30-35.
- [9] R. Remy, Statistical Quality Control and Process Capability Analysis for Variability Reduction of the Tomato Paste Filling Process,Industrial Engineering & Management Journal, (2014).

Measurement of Residual Stresses of Al/Mg Compounds by the Hole-Drilling Strain Gage Method with MATLAB Package(RSHDM)

Ass. Prof. Dr. Abdullah Dhayea Assi¹, Lecturer Dr.Safaa M. Hassoni²

Lecturer Ahmed Jasim Mohammed³, Lecturer Ameer H. Sabry⁴

^{1,2} Institute of Technology/Baghdad, ³Alswera Technology Institute, ⁴Ministry of Electricity/ Al-Quds Power Plant

ABSTRACT

The residual stress analyses of Al/Mg compounds were done using the hole drilling method with strain gage rosettes. The evaluation method used is based on an MATLAB Package, which includes the analyses of the residual stress state when using an (PC/ interactive WinDaq program) to calculate strains which is measured by the strain gage rosettes. The results of the hole drilling show examples of strain distributions versus the hole depth for specimen heights ((h) of 20 and 5 mm). The experimental results reveal that the strain curves depend on the specimen height, even a change in sign can be demonstrated. Also it was found that the largest residual stress is affecting the axial component as a compressive stress near the inner surface and a tensile stress near the outer surface.

KEYWORDS:

Al/Ma Compound, Residual Stress, Hole Drilling Method, Strain Gage Rosette, MATLAB, RSHDM.

NOMENCLATURES

\bar{a}, \bar{b}	Coefficients for micro-measurements residual stress rosettes	σ_0	Nominal stress
\bar{A}, \bar{B}	Experimental coefficients	σ_x	Longitudinal residual stress
D	Rosette mean diameter	σ_y	Transverse residual stress
Do	Die input diameter	α	Angle of orientation of the main stress
Do	Hole diameter	γ_{xy}	Shear strain
Do/D	Ratio of hole diameter to gage circle diameter	$\epsilon_1, \epsilon_2,$	Deformations measured by strain gauges 1,2,3
p	$(\epsilon_3 + \epsilon_1)$	ϵ_3	Strain in x- direction
q	$(\epsilon_3 - \epsilon_1)$	ϵ_x	Strain in y- direction
s	Specimen thickness	σ_{max}	Maximum principal stress
v	Poisson's ratio	σ_{min}	Minimum principal stress

ARTICLE INFO

Received 7 August 2018

Accepted 11 October 2018

DOI: 10.xxxxx

ISSN: 2413-0230

AL-MUHANDIS Journal (JMISE)

© 2018 Iraqi Society of Engineers (ISE)

E-mail: jmise@ise-iq.org

Online: www.jmise.ise-iq.org

Office Address: Iraq, Baghdad, Al-Nidhal Q., 103-30-5

CORRESPONDING AUTHOR

Name: Ass. Prof. Dr. Abdullah Dhayea Assi

Email: drabdullah_dhayea@yahoo.com

Research Field:

Google Scholar:

1. INTRODUCTION

Residual or internal stresses are the system of stresses which can exist in a body when it is free from all external forces, couples, and applied stresses. The presence of residual stresses in the proper manner will greatly improve the design criterion of the strength-to-weight ratio and reduce the final cost. However, residual stresses are often associated with warping and distortion after heat treatment or machining, and early service failures of tools, dies, machine parts, and welded members [1]. Drew V. Nelson[2],claim that residual stresses in an elastic solid arise from three distinct sources, namely, misfit, change in specific volume, and non-uniform distortion.

The hole-drilling method is one of the most well-known methods for measuring residual stresses. To identify unknown plane stresses in a specimen, a circular hole is first drilled in the infinite plate under plane stress, then the strains resulting from the hole drilling is measured, Mathar [3].

The aim this work is constructing a rig to measure the strains from which the residual stresses, can be calculated by using a specialized computer program in order to completely elimination of the compute labor MATLAB package.

2. THEORETICAL ANALYSIS

A. The hole Drilling Method Analysis (Rectangular Rosette)

Assume that the principal strains at the rectangular rosette are oriented at an angle, ϕ , $\epsilon_x = \epsilon_1$ and $\epsilon_y = \epsilon_2$ and compute ϵ_x , for angles of rotation ϕ , $\phi+45^\circ$, and $(\phi+90^\circ)$ to yield three equations as show in fig.(1) [5]:

$$\epsilon_A = \frac{\epsilon_1 + \epsilon_2}{2} + \frac{\epsilon_1 - \epsilon_2}{2} \cos 2\phi \dots\dots\dots(1a)$$

$$\epsilon_B = \frac{\epsilon_1 + \epsilon_2}{2} + \frac{\epsilon_1 - \epsilon_2}{2} \cos 2(\phi + 45) \dots\dots\dots(1b)$$

$$\epsilon_C = \frac{\epsilon_1 + \epsilon_2}{2} + \frac{\epsilon_1 - \epsilon_2}{2} \cos 2(\phi + 90) \dots\dots\dots(1c)$$

These are 3 simultaneous equations relating to $\epsilon_A, \epsilon_B, \epsilon_C$ to $\epsilon_1, \epsilon_2, \phi$. It is a relatively simple matter to invert the equations and solve for $\epsilon_1, \epsilon_2, \phi$ in terms of $\epsilon_A, \epsilon_B, \epsilon_C$ yielding [5]:

$$\epsilon_{1,2} = \frac{\epsilon_A - \epsilon_C}{2} \pm \frac{1}{\sqrt{2}} \sqrt{(\epsilon_A - \epsilon_B)^2 + (\epsilon_A - \epsilon_C)^2} \dots\dots(2a,b)$$

$$\phi = \frac{1}{2} \tan^{-1} \left(\frac{\epsilon_A - 2\epsilon_B + \epsilon_C}{\epsilon_C - \epsilon_A} \right) \dots\dots\dots(2c)$$

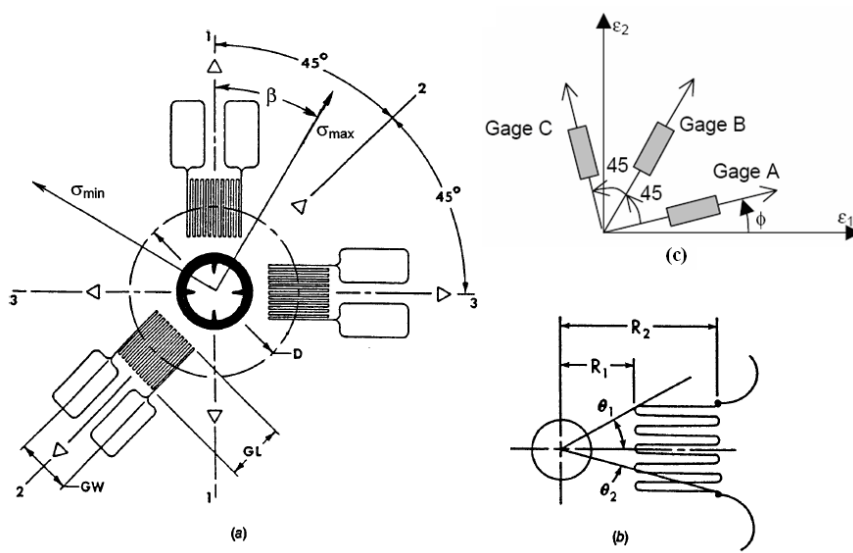


Figure (1): Rectangular Rosette Gage Orientation [5]

B. The Stress Components

Where the basic coefficients **A & B** obtained from a equations,[5]:

$$\bar{A} = -\frac{\bar{a}(1+\nu)}{2E} \quad \dots(3a) \quad \&$$

$$\bar{B} = -\frac{\bar{b}}{2E} \quad \dots\dots\dots(3b)$$

The principal stresses and their direction, the results can be expressed as:

$$\sigma_{\max} = \frac{\epsilon_1 + \epsilon_3}{4A} - \frac{1}{4B} \sqrt{(\epsilon_3 - \epsilon_1)^2 + (\epsilon_3 + \epsilon_1 - 2\epsilon_2)^2} \quad \dots(4a)$$

$$\sigma_{\min} = \frac{\epsilon_1 + \epsilon_3}{4A} + \frac{1}{4B} \sqrt{(\epsilon_3 - \epsilon_1)^2 + (\epsilon_3 + \epsilon_1 - 2\epsilon_2)^2} \quad \dots(4b)$$

Where α is the angle from the nearer principal axis to gage no.1 (in the direction of gage numbering, if positive; or opposite, if negative). Reversing the sense of α to more conveniently defines the angle from gage No.1 to the nearer axis, while retaining the foregoing sign convention,[5],

$$\tan 2\alpha = \frac{\epsilon_1 - 2\epsilon_2 + \epsilon_3}{\epsilon_1 - \epsilon_3} \quad \dots\dots\dots(4c)$$

And the maximum shear stress is:

$$\tau_{\max} = \frac{\sigma_{\max} - \sigma_{\min}}{2} = \mp \frac{1}{4B} \sqrt{(\epsilon_3 - \epsilon_1)^2 + (\epsilon_3 + \epsilon_1 - 2\epsilon_2)^2} \quad \dots(4d)$$

The Data-Reduction Procedures of Residual Stress Determination is to calculate the relieved strain parameters $(\epsilon_3 + \epsilon_1)/2$ and $(\epsilon_3 - \epsilon_1)/2$ at each depth increment . The residual stress will first be calculated using only the maximum measured strains at the full-hole depth (Z= 4 mm). Then:

D =10 mm and Do =3 mm then Do/D =0.3
 Z =[0.5 1 1.5 2 2.5 3 4] mm & Z/D
 =[0.05 0.1 0.15 0.2 0.25 0.3 0.4]

Three different groups of relieved strains appear in symbols(p, q and t) . These are the mean hydrostatic strain p, the tensor shear strain 45° to gage 1 axis q, and the tensor shear strain along gage 1 axis t. These strains are given by Equations below [5]:

$$p = \frac{(\epsilon_3 + \epsilon_1)}{2} \quad \dots\dots\dots(5a)$$

$$q = \frac{(\epsilon_3 - \epsilon_1)}{2} \quad \dots\dots\dots(5b)$$

$$t = \frac{(\epsilon_3 + \epsilon_1 - 2\epsilon_2)}{2} \quad \dots\dots\dots(5c)$$

when an x-y coordinate system is established such that the x direction is parallel to the gage 1 axis, then the stress quantities corresponding to the p, q, and t strains are :

$$P = \frac{p}{2.A} \quad \dots\dots\dots(6a)$$

$$Q = \frac{q}{2.B} \quad \dots\dots\dots(6b)$$

$$T = \frac{t}{2.B} \quad \dots\dots\dots(6c)$$

Where P is the mean hydrostatic stress, Q is the shear stress 45° to x-y axes, and T is the shear stress along the x-y axes. Once the stresses P, Q, and T have been calculated, all principal and conventional stress quantities can be found using [5]:

$$\sigma_x = P - Q \quad \dots\dots\dots(7a)$$

$$\sigma_y = P + Q \quad \dots\dots\dots(7b)$$

$$\tau_{xy} = T \quad \dots\dots\dots(7c)$$

The τ_{xy} can be eliminated from Eqs. (7a) and (7b) using Eq. (7c)). Therefore, the resulting Eqs. (8a) and (8b) can be solved simultaneously to calculate σ_x and σ_y , which can then be used to calculate τ_{xy} [5]:

$$\sigma_{\max} = \frac{\sigma_x + \sigma_y}{2} + \frac{\sigma_x - \sigma_y}{2} \cdot \cos 2\beta + \frac{\sigma_x - \sigma_y}{2} \cdot \tan 2\beta \cdot \sin 2\beta \quad \dots(8a)$$

$$\sigma_{\min} = \frac{\sigma_x + \sigma_y}{2} - \frac{\sigma_x - \sigma_y}{2} \cdot \cos 2\beta - \frac{\sigma_x - \sigma_y}{2} \cdot \tan 2\beta \cdot \sin 2\beta \quad \dots(8b)$$

$$\tau_{\max} = \frac{\sigma_{\max} - \sigma_{\min}}{2} \quad \dots(8c)$$

Adding Eq. (7) and (8) results in:

$$\sigma_{\max} + \sigma_{\min} = \sigma_x + \sigma_y \quad \dots\dots\dots(9)$$

Which is the stress invariant and the transformed stresses must satisfy k. Equation (8) can be used to verify that the transformation was performed correctly.

3. THE PACKAGE RSHDM BY MATLAB

The Layout Editor (along with the Toolbar Editor and Icon Editor) to create menus and toolbars, create and modify tool icons, and set basic properties of the

GUI components as shown in Figure(2). To get started, use the Layout Editor and setting property values, see Creating a Simple GUI with GUIDE in the MATLAB Creating Graphical User Interfaces documentation as shown in figure(3).

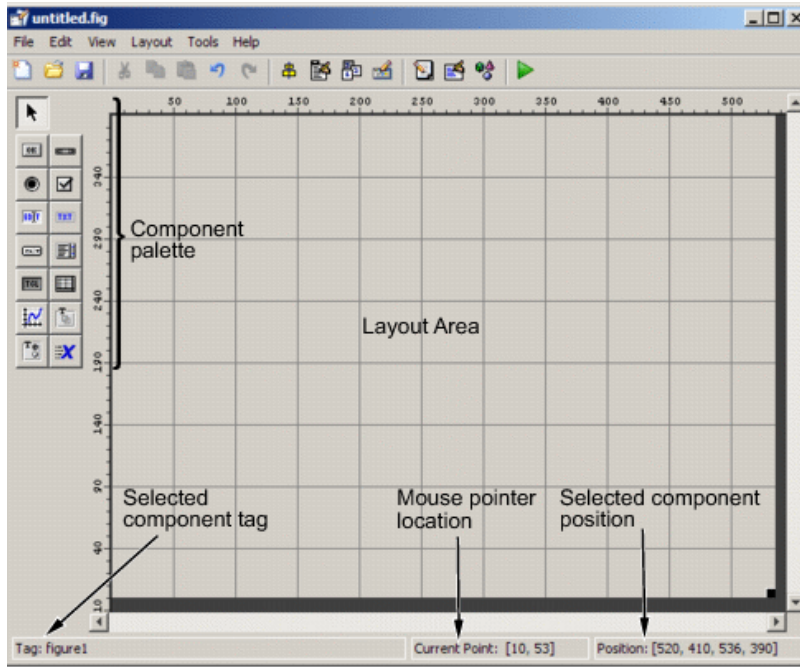


Fig.(2): The Layout Editor(GUI)Graphical User Interfaces[8]

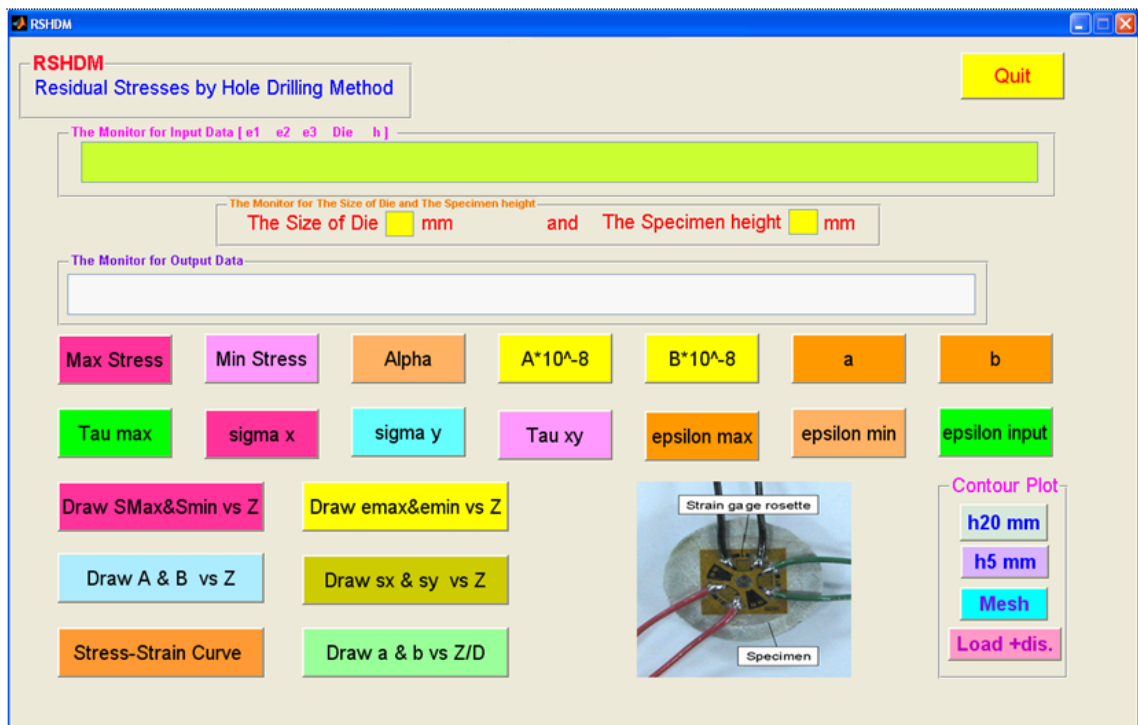


Fig.(3): Package for Estimation Residual stresses by Hole Drilling Method

1- Title of Package is (RSHDM)

It means (Residual Stresses by Hole Drilling Method)

2- The Monitor for input data

The monitor is used to input data by matrix notation in form :

$$e = [e1 \ e2 \ e3 \ Die \ h]$$

$e1$ =Component strains at gage No.1

$e2$ =Component strains at gage No.2

$e3$ =Component strains at gage No.3

Die = The size of Die where found three size for Die (45 , 40 and 35) respectively.

h = The specimen height where two specimens height (h=20mm & h=5mm)

Example of input data: if size is of Die=45 mm and specimen height h=20mm . Also:

$$\epsilon1 = \epsilon90 = e1 = [24 \ 43 \ 54 \ 61 \ 66 \ 70 \ 73]$$

$$\epsilon2 = \epsilon45 = e2 = [19 \ 33 \ 44 \ 48 \ 51 \ 53 \ 54]$$

$$\epsilon3 = \epsilon0 = e3 = [18 \ 31 \ 38 \ 42 \ 45 \ 47 \ 48]$$

Then input the line vector only in the Monitor for input data:

e =

$$[24 \ 43 \ 54 \ 61 \ 66 \ 70 \ 73 \ 19 \ 33 \ 44 \ 48 \ 51 \ 53 \ 54 \ 18 \ 31 \ 38 \ 42 \ 45 \ 47 \ 48 \ 45 \ 20]$$

Also the dialog message is shown in case it runs without data .This message is ((Input must be a Data Vector)) as shown in figure (4).

3- The monitor for the size of die and specimen height

Where in this monitor values of die size and specimen height are shown in order to be sure input values are correct .

4- The monitor for output data

This monitor is used to show results for any variable.

5- Calculate The Variables

- Max stress : To calculate the maximum principal residual stress use equation (4a).
- Min stress: To calculate the minimum principal residual stress use equation (4b).
- Alpha : where (Alph = α) is the angle from the nearer principal axis to gage No.1.To calculate α using equation(4c).
- Tau max : To calculate the maximum shear stress using equation (4d).
- Calibration Coefficients (a and b)

The calibration coefficient \bar{a} & \bar{b} are dimensionless, almost material-independent

constants. The program (RSHDM) converts \bar{a} & \bar{b} from figure to table.

- The material coefficients \bar{A} & \bar{B}
After obtain dimensionless coefficient \bar{a} & \bar{b} we can be calculate the material coefficients \bar{A} & \bar{B} by using equation (3a) to get \bar{A} and using equation (3b) to get \bar{B} .
- Sigma x , sigma y and Tau xy
Sigma x = σ_x =The stress component at direction of x.
Sigma y = σ_y =The stress component at direction of y.

Tau xy = τ_{xy} = The shear stress in plane xy.

To calculate the variables you must determent p , q and t then P , Q and T thereupon you get this variables. Then :

$$p = \text{the mean hydrostatic strain} = (\epsilon3 + \epsilon1) / 2 ; (5a)$$

$$q = \text{the tensor shear strain } 45^\circ \text{ to gage No. 1 x-y axes} = (\epsilon3 - \epsilon1) / 2 ; (5b)$$

$$t = \text{the tensor shear strain along gage-1 x-y axes} = (\epsilon3 + \epsilon1 - 2\epsilon2) / 2 ; (5c), \text{ and}$$

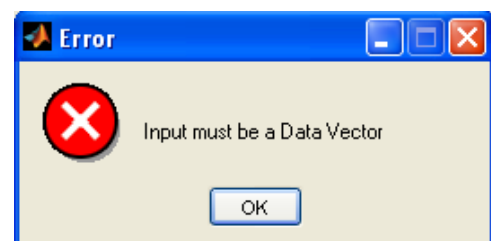


Fig.(4): Dialog box when it runs without data

$$P = \text{the mean hydrostatic stress} = p / 2A ; (6a)$$

$$Q = \text{the shear stress } 45^\circ \text{ to x-y axes} = q / 2B ; (6b)$$

$$T = \text{the shear stress along the x-y axes} = t / 2B ; (6c)$$

Once the stresses P, Q, and T have been calculated, all principal and conventional stress quantities can be found using equation (7a,b,c):
 $\sigma_x = P - Q$, $\sigma_y = P + Q$ & $\tau_{xy} = T$

h- Epsilon max and epsilon min

To calculate the maximum principal strain (ϵ_{max}) use equation (2a) and the maximum principal strain (ϵ_{min}) by use equation(2b).

i- Epsilon input

This icon shows input data for component strains only in order to be sure input values for strains are correct: [24 43 54 61 66 70 73 19 33 44 48 51 53 54 18 31 38 42 45 47 48]

6- Plot the curves

- a- Draw σ_{max} & σ_{min} vs Z: draw the maximum and minimum principal residual stresses versus hole depth (Z) to show side in window as shown in figure(5).
- b- Draw ϵ_{max} & ϵ_{min} vs Z: draw the maximum and minimum principal strains versus hole depth (Z) to show side in window as shown in figure(5).
- c- Draw A & B vs Z : draw the material coefficients \bar{A} & \bar{B} versus hole depth (Z) to show side in window as shown in figure(5).
- d- Draw σ_x & σ_y vs Z: draw (σ_x)The stress component at the direction of x and (σ_y)The stress component at the direction of y versus hole depth (Z) to show side in window as shown in figure(5).
- e- Stress-Strain Curve: draw the maximum and minimum principal residual stresses versus the maximum and minimum principal strains to show side in window as shown in figure(5).
- f- Draw a & b vs Z/D : draw the dimensionless coefficient \bar{a} & \bar{b} versus the dimensionless hole depth (Z/D) to show side in window as shown in figure(5).

7- Contour Plot

If you press on icon (h20 mm) contour plot of specimen height 20 mm will appear to show side in window as shown in figure(5) and you press on icon (h5 mm) will be contour plot for specimen height 5 mm will appear to show side in window as shown in figure(5). If you press in reverse (i.e the data input for h20mm and press on icon h5mm and vice versa) hence the dialog gives message in the window for output data is ((The Specimen height is wrong)).

8- (Mesh)

If you press on icon (Mesh) you plot the meshing for specimen height input to show side in window as shown in figure(5).

9- (Load + displacement)

If you press on icon (Load + dis.) you plot the Load and displacement for specimen height input to show side in window as shown in figure(5).

10- (Quit)

To exit package press on icon (Quit).

4- LAY OUT OF THE PACKAGE FOR RSHDM AFTER RUN

The input is data for the size of die 45 mm and the specimen height h=20 mm and you press on icon(Max Stress) ; also then press on icon (Stress-Strain Curve).

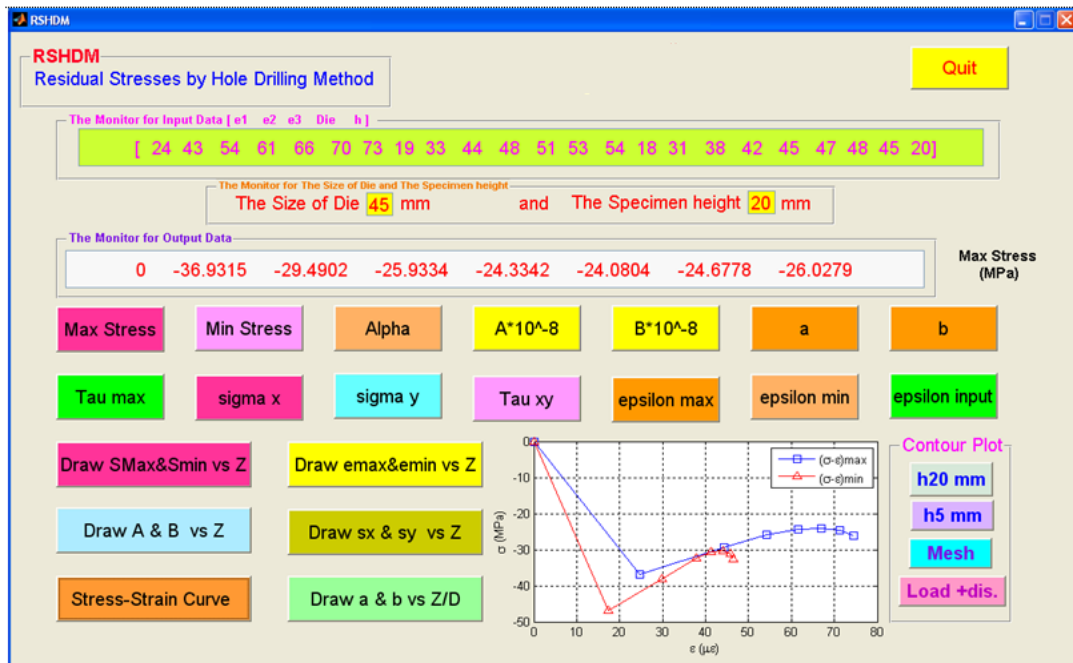


Fig.(5): This figure at Run (press icon{Max stress}and icon{stress-strain curve})

5. EXPERIMENTAL WORK

The commercial Aluminum of AlMgSi1 (DIN 1725-1) which is used in the electrical industry was used as a billet. These tests were made in Special Institute for Engineering Industries (SIEI). The chemical composition of this material is illustrated in Table (1) and the mechanical properties in Table (2).

The commercial magnesium criterion is (AZ63A) from (SAE AMS4420) which is used in the typical tubes. These tests were made in Special Institute for Engineering Industries (SIEI). The chemical composition of this material is illustrated in Table (3) and the mechanical properties in Table (4).

Table(1): The chemical composition of aluminum of AlMgSi1 (DIN 1725-1)

Element%	Si	Fe	Cu	Mn	Mg	Zn	V	AL
Standard	1.12	0.3	0.3	0.424	0.923	0.026	0.003	96.9
Experimental	1.18	0.34	0.36	0.5	0.972	0.039	0.009	96.6

Table (2):The mechanical properties of aluminum of AlMgSi1 (DIN 1725-1)

Properties	σ_u (MPa)	σ_y (MPa)	Elongation (mm)	E (GPa)	Poission's ratio	HV	HB	density (kg/m ³)
Standard	310	260	10	70	0.3	61	106	2700
Experimental	315	270	12	70	0.3	65	110	2700

Table (3): The chemical composition of magnesium of AZ63A

Element%	Al	Cu	Mn	Ni	Si	Zn	Total others	Mg
Standard	6	0.1	0.15	0.01	0.3	3.04	0.4	90
Experimental	5	0.2	0.2	.03	0.4	2.01	0	92.16

Table (4):The mechanical properties of the commercial magnesium of AZ63A

Properties	σ_u (MPa)	σ_y (MPa)	Elongation (mm)	E (GPa)	Poission's ratio	HV	HB	density (kg/m ³)
Standard	151	76	4	45	0.33	33	75	1738
Experimental	155	80	6	45	0.33	35	78	1738

The residual stress rosettes described previously impose no special instrument requirements, readily accessible form. A special software Windows-based computer program (WinDaq) is also available to perform and calculate residual stress magnitudes in accordance with ASTM E837 [6]. The database for the program includes values of the coefficients

\bar{a} & \bar{b} for blind holes, and covers the full range of recommended hole dimensions applicable to all micro-measurements of residual stress rosettes [6]. The strain gages rosettes and measurement positions are shown in Figure (6) and the three joint parts of strain gage rosettes are shown in Figure (7).

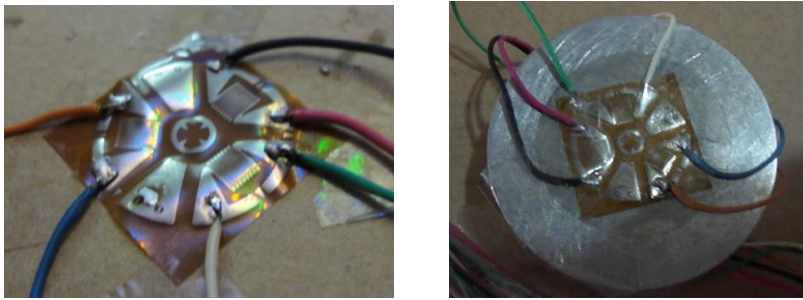
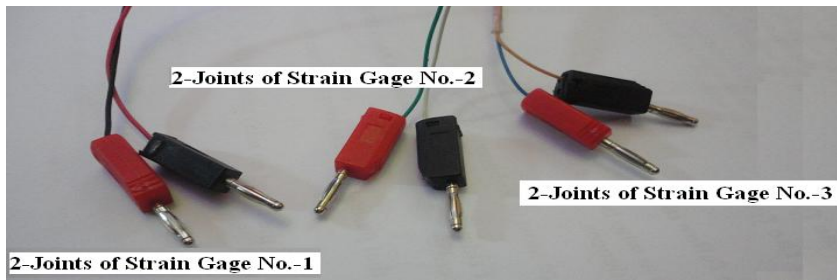


Figure (6): Strain gages rosettes and measurement positions



Figure(7): The three joint parts of strain gage rosettes

The 8-Channels Strain Measuring quarter bridge circuit with (WinDaq software) data acquisition device and computer are shown in Figure (8).

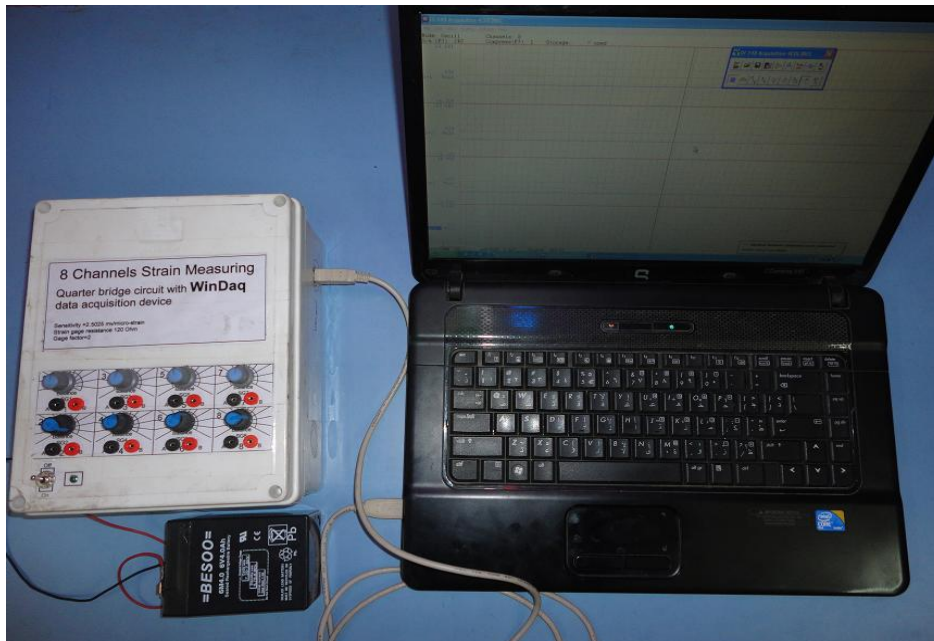


Figure (8): 8-Channels Strain Measuring (WinDaq) device and computer

6. RESULTS AND DISSECTION

The strain sensitivity of the hole-drilling method is typically quite modest. Low strain sensitivity can diminish the reliability of the calculated residual stresses by reducing the size of the measured strains relative to that of the strain measurement errors. The strain sensitivity, is defined as the relieved strain per unit residual stress, and is quantified through the calibration coefficients \bar{a} and \bar{b} . Larger calibration coefficients are desirable because they indicate higher strain sensitivity, and hence greater resistance to the effects of strain measurement errors.

6.1 The Uniform-Stress Coefficient (\bar{a} & \bar{b})

The values of \bar{a} & \bar{b} (or \bar{A} & \bar{B}) are low because the strain gages are located at the some distance from the hole. The material underneath the

gages is subjected only to partial strain relief. If it were possible to relieve completely the strains in the material under all the gages, then it may be shown from Hook's law that the corresponding calibration coefficients would be [5]:

$$\text{maximum value of } \bar{a} = \frac{1-\nu}{1+\nu} = 0.54 \text{ for } \nu = 0.3$$

$$\text{maximum value of } \bar{b} = 1+\nu = 1.3 \text{ for } \nu = 0.3$$

Figures (9a)&(9b) shows that for the traditional straight hole, the maximum values for \bar{a} & \bar{b} are at most only half of the full strain relief values. Thus, significant scope exists for increasing the strain sensitivity of the strain measurements.

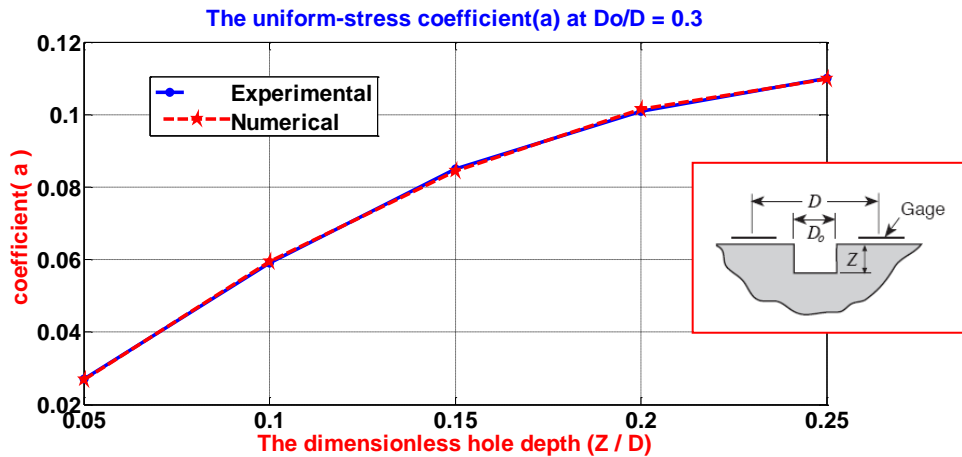


Fig.(9a): The uniform-stress coefficient (a) versus the dimensionless hole depth (Z/D) at (Do/D)

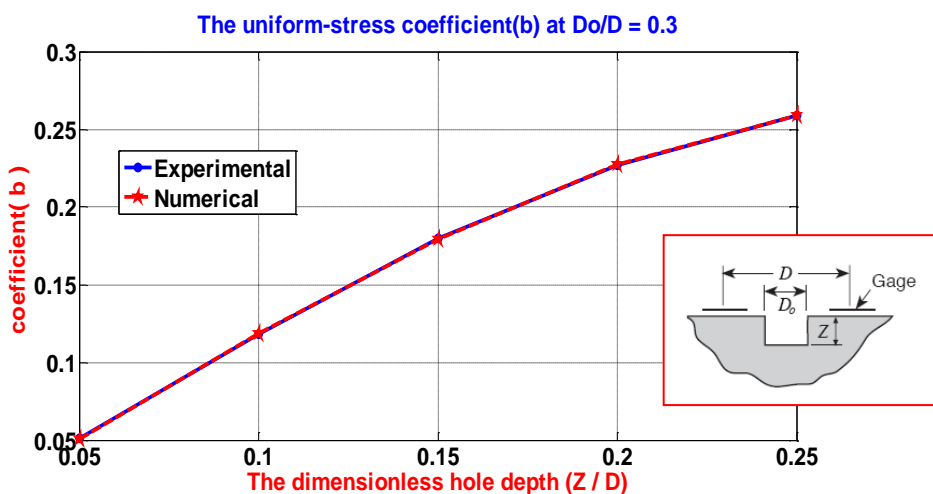
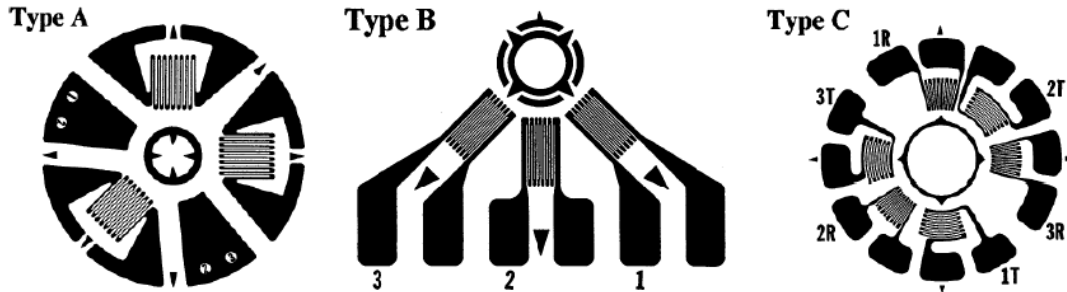


Fig.(9b):The uniform-stress coefficient (b) versus the dimensionless hole depth (Z /D) at (Do/D)

Calibration constants for blind and through hole in thick and thin specimens have been evaluated for all the types of strain gage rosettes available on the market. The calculated calibration constants are helpful to increase the precision of the residual stress

evaluation with the MATLAB software. The ASTM E837[6] standard takes into consideration three different kinds of rosette figure(10), indicated as kind A, B and C.



Figure(10): Strain gage rosettes used in ASTM E837[5]

Table 5: Calibration constants for Rosette A

Rosette A	\bar{a}					\bar{b}				
Blind hole	Do/D					Do/D				
Z / D	0.30	0.35	0.40	0.45	0.50	0.30	0.35	0.40	0.45	0.50
0.00	0.000	0.000	0.000	0.000	0.000	0.000	0.000	0.000	0.000	0.000
0.05	0.027	0.037	0.049	0.063	0.080	0.051	0.069	0.090	0.113	0.140
0.10	0.059	0.081	0.108	0.138	0.176	0.118	0.159	0.206	0.255	0.317
0.15	0.085	0.115	0.151	0.192	0.239	0.180	0.239	0.305	0.375	0.453
0.20	0.101	0.137	0.177	0.223	0.273	0.227	0.299	0.377	0.459	0.545
0.25	0.110	0.147	0.190	0.238	0.289	0.259	0.339	0.425	0.513	0.603
0.30	0.113	0.151	0.195	0.243	0.293	0.279	0.364	0.454	0.546	0.638
0.35	0.113	0.151	0.195	0.242	0.292	0.292	0.379	0.472	0.566	0.657
0.40	0.111	0.149	0.192	0.239	0.289	0.297	0.387	0.482	0.576	0.668
Through hole	0.090	0.122	0.160	0.203	0.249	0.288	0.377	0.470	0.562	0.651

6.2 THE MATERIAL COEFFICIENTS (\bar{A} & \bar{B})

There are no convenient analytical value for the calibration coefficients \bar{A} & \bar{B} . for this case, values of \bar{A} & \bar{B} are obtained either experimentally or numerically. The calibration coefficients can be determined. The experimental calibration has the advantage of conceptual simplicity and accounting for the procedural influences and material-dependent effects on measured strain response. One disadvantage is that a separate time consuming calibration is needed for every material, hole size, and rosette geometry.

Numerical determination of the calibration coefficients \bar{A} & \bar{B} was made possible by the development of the finite element method . as shown as in figures(11&12).

The procedure described here was applied to a through hole specimen made from Compound cylinders (AlMgSi1/AZ63AMg, this geometry (Do/D = 0.38) the hole is normally drilled to a depth corresponding to at least Z/D = 0.4 (ASTM E 837[6,7] specifies Z/D = 0.4 for the maximum hole depth).

It should be noted that the values for the basic coefficients \bar{A} & \bar{B} obtained from a particular calibration test are strictly applicable only to residual-stress measurement conditions that exactly match the calibration conditions [3,7]:

- ✚ material with the same elastic properties;
- ✚ same rosette geometry (but rosette orientation is arbitrary);
- ✚ same hole size.

Numerical calibration is more general and covers a wide range of measurement condition. Numerical calibration closely matches the experimental

calibration, and is widely accepted and used, as shown as in figures(11&12).

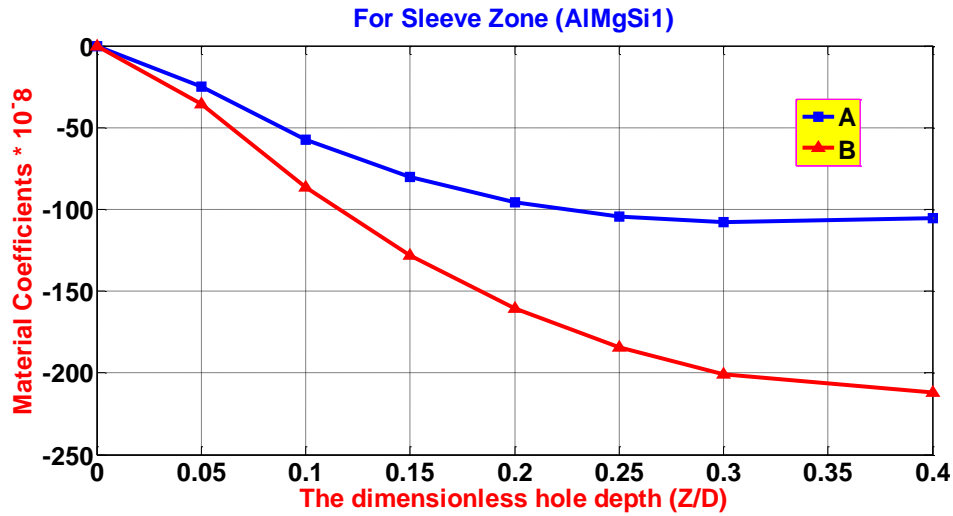


Fig.(11): The Material Coefficients (\bar{A} & \bar{B}) versus The dimensionless hole depth (Z/D) for Sleeve

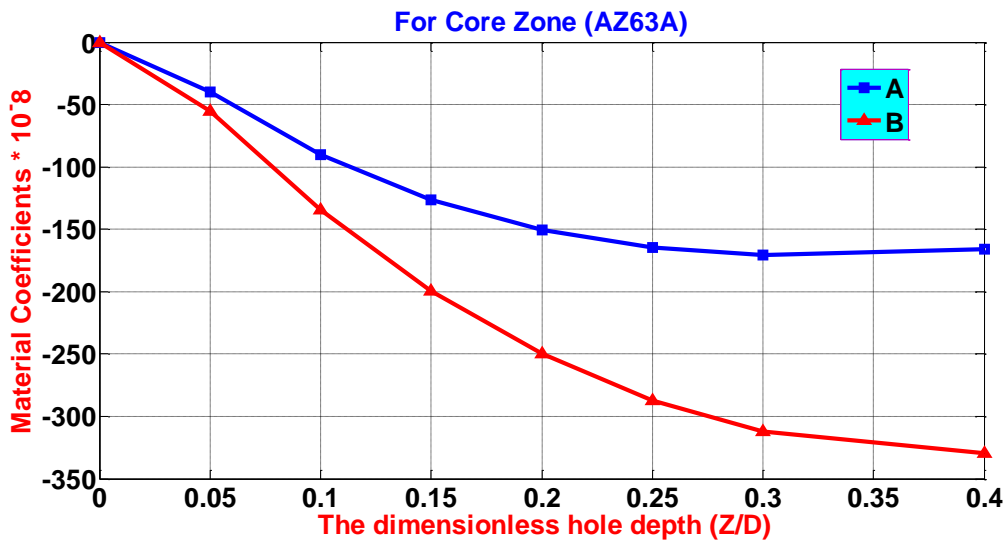


Fig.(12): Material Coefficients (\bar{A} & \bar{B}) versus The dimensionless hole depth (Z/D) for core

7. THE RESIDUAL STRESSES RESULTS

The results of the residual stresses are summary in tables(6a 1& 2).

Table (6a1): Residual Stress Determination for Die 45 mm at Specimen height 20 mm

Die45h20		mVolt	Measured Strain			Relieved Strains			Coefficients Multiplier			α degree	EUS to Depth Z		
Z (mm)	Z/D		$(\mu\epsilon = mV/2.5025)$ ($\mu\epsilon$)			$\epsilon_3 + \epsilon_1$	$\epsilon_3 - \epsilon_1$	$\epsilon_3 + \epsilon_1 - 2\epsilon_2$	From curve		A&B ($\times 10^3$)		σ_{max} (MPa)	σ_{min} (MPa)	
0	0	0	E1	0	0	0	0	0	a	0	A	0	0	0	0
		0	E2	0	%	%	%								
		0	E3	0	0	0	0	b	0	B	0				
0.5	0.05	60.06	E1	24	42	-6	4	a	0.027	A	-25.07	-16.9	-36.94	-46.83	
		47.55	E2	19	%	%	%								
		45.05	E3	18	34.71	24.00	30.77	b	0.051	B	-36.42				
1	0.1	107.61	E1	43	74	-12	8	a	0.059	A	-54.78	-16.9	-29.50	-38.05	
		82.58	E2	33	%	%	%								
		77.6	E3	31	61.16	48.00	61.54	b	0.118	B	-84.28				
1.5	0.15	135.14	E1	54	92	-16	4	a	0.085	A	-78.92	-7.1	-25.94	-32.35	
		110.11	E2	44	%	%	%								
		95.10	E3	38	76.03	64.00	30.77	b	0.180	B	-128.57				
2	0.2	152.65	E1	61	103	-19	7	a	0.101	A	-93.78	-10.2	-24.34	-30.58	
		120.12	E2	48	%	%	%								
		105.11	E3	42	85.12	76.00	53.85	b	0.227	B	-162.14				
2.5	0.25	165.17	E1	66	111	-21	9	a	0.110	A	-102.14	-11.6	-24.09	-30.26	
		127.63	E2	51	%	%	%								
		112.61	E3	45	91.74	84.00	69.23	b	0.259	B	-185				
3	0.3	175.175	E1	70	117	-23	11	a	-	A	-	-	Beyond Range	-	
		132.63	E2	53	%	%	%								
		117.62	E3	47	96.69	92.00	84.62	b	-	B	-				
4	0.4	182.68	E1	73	121	-25	13	a	0.111	A	-103.07	-13.8	-26.02	-32.67	
		135.14	E2	54	%	%	%								
		120.12	E3	48	100	100	100	b	0.297	B	-212.14				
1	2	3	4			5	6	7	8		9	10	11	12	

Table(6a2): Residual Stress Determination for Die 45 mm at Specimen height 20 mm

Die45h20		Max Shear Stress τ_{max} (MPa)	Relieved Strains			Component Stresses (MPa)	Relieved Strains max & min															
Z (mm)	Z/D		$(\mu\epsilon)$				(MPa)	ϵ_{max} (%)	ϵ_{min} (%)													
0	0	0	p	0	0	0	0	0	0	0	0	0	0									
			q	0										0	0	0	0	0	0			
			t	0																		
0.5	0.05	4.95	p	21	34.71	24.00	30.77	P	-41.89	σ_x	-47	24.61	17.40									
			q	-3										34.71	24.00	30.77	Q	4.12	σ_y	-38.6	%	%
			t	2																		
1	0.1	4.28	p	37	61.16	48.00	61.54	P	-33.77	σ_x	-36.6	44.22	29.79									
			q	-6										61.16	48.00	61.54	Q	3.56	σ_y	-29.7	%	%
			t	4																		
1.5	0.15	3.21	p	46	76.03	64.00	30.77	P	-29.15	σ_x	-32.5	54.25	37.76									
			q	-8										76.03	64.00	30.77	Q	3.12	σ_y	-26.3	%	%
			t	2																		
2	0.2	3.13	p	51.5	85.12	76.00	53.85	P	-27.46	σ_x	-30.6	61.63	41.38									
			q	-9.5										85.12	76.00	53.85	Q	2.93	σ_y	-24.7	%	%
			t	3.5																		
2.5	0.25	3.09	p	55.5	91.74	84.00	69.23	P	27.17	σ_x	-30.1	66.93	44.08									
			q	-10.5										91.74	84.00	69.23	Q	2.84	σ_y	-24.4	%	%
			t	4.5																		
3	0.3	-	p	58.5	96.69	92.00	84.62	P	-27.88	σ_x	-	Beyond Range	-									
			q	-11.5										96.69	92.00	84.62	Q	2.89	σ_y	-	-	-
			t	5.5																		
4	0.4	3.33	p	60.5	100	100	100	P	-29.4	σ_x	-1.54	74.59	46.42									
			q	-12.5										100	100	100	Q	2.95	σ_y	-26.5	%	%
			t	6.5																		
1	2	13	14	15	16	17	18	19	20	21												

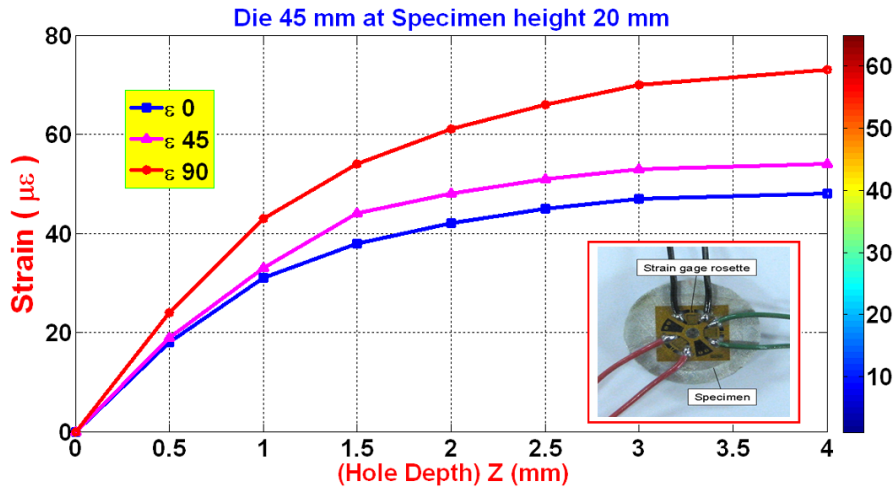


Figure (13): Strain(ε) versus Hole depth (Z)

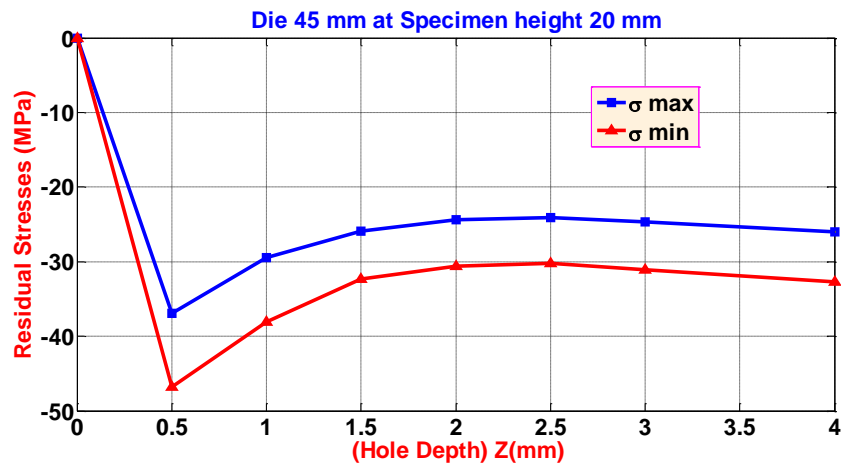


Figure (14): Residual Stresses versus Hole depth (Z)

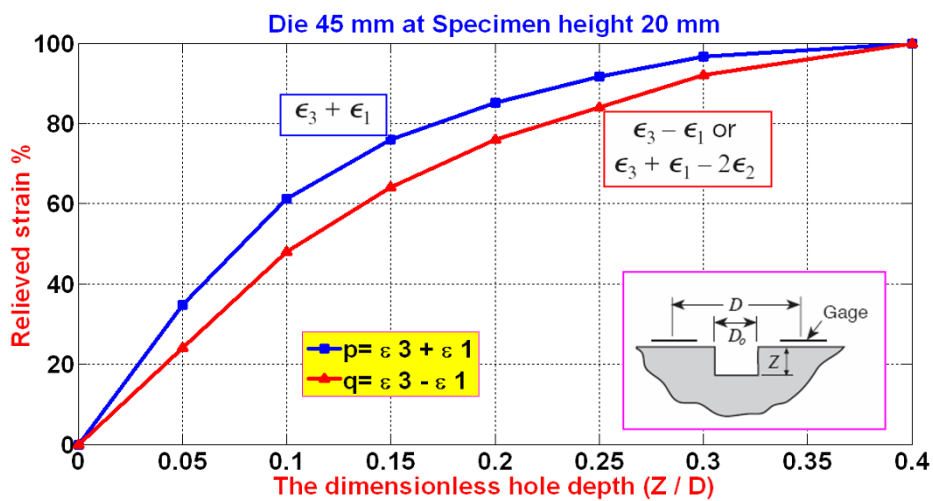


Figure (15): Relieved Strain (%) versus the dimensionless hole depth (Z/D)

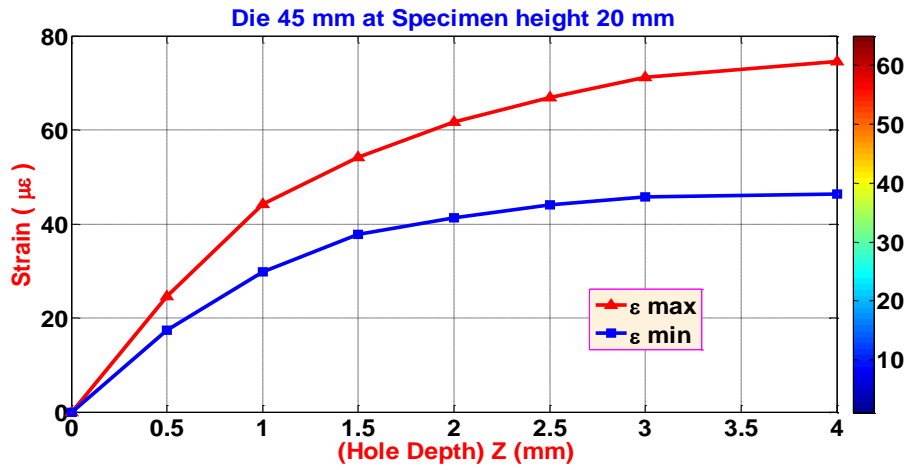


Figure (16): Strain(ϵ_{max} & ϵ_{min}) versus Hole depth (Z)

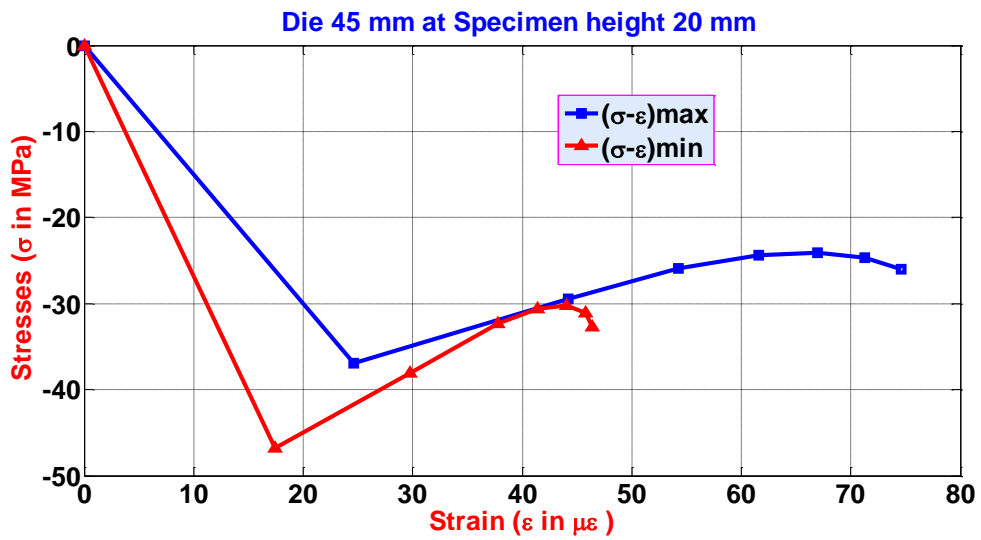
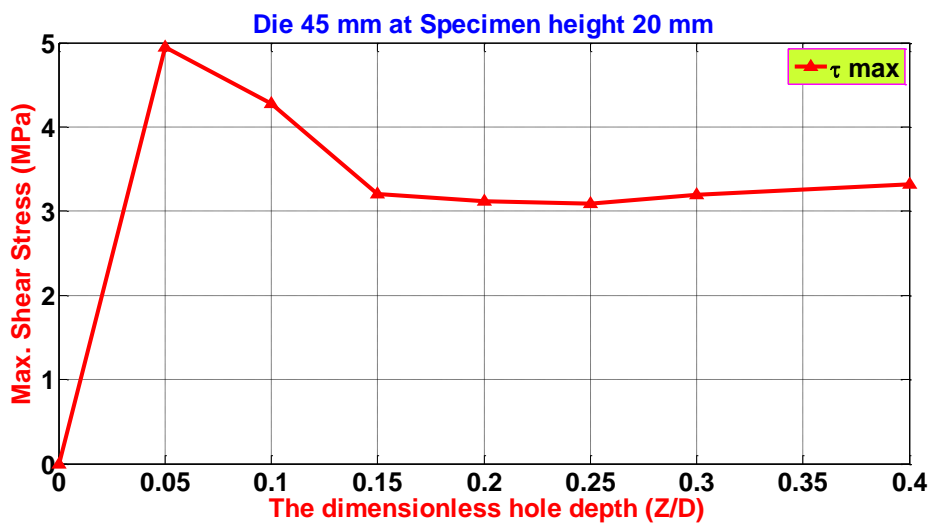


Figure (17): Residual Stresses (σ) versus Strain (ϵ)



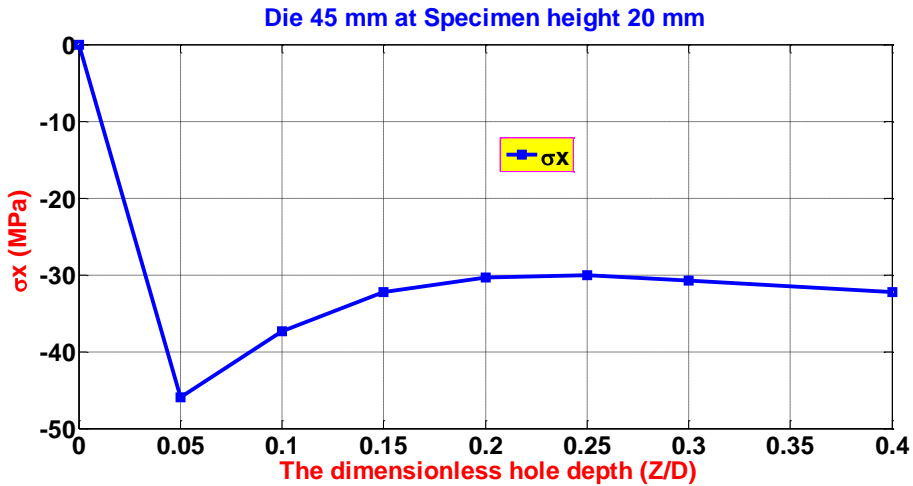


Figure.(19): σ_x versus The dimensionless Hole depth (Z/D)

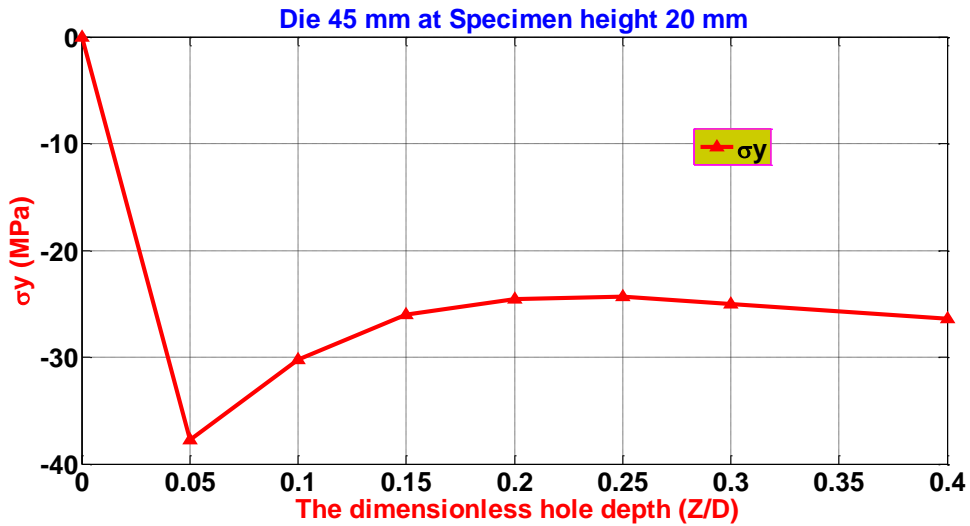


Figure.(20): σ_y versus The dimensionless Hole depth (Z/D)

Figs.(13-20) from several test series, it was proved that the characteristic of the strain distributions is reproducible. Hence, it can be demonstrated that the real residual stress state is approximated by the numerically determined stress distribution. That is, the formation of residual stresses is dominated by the cooling process and the elasticity of material behavior.

8. CONCLUSIONS:

First, a comprehensive study of the various techniques used to measure residual stresses in Al/Mg compound was carried out. From the present study, the most appropriate techniques to measure residual stresses for the specimen (Al / Mg) considering its geometrical shape of die is the hole drilling technique

On the other hand another approach for analysis is modeling and simulation which studies a special numerical for the cooling process via different

coefficients of thermal expansion at the compound or the materials .

Several main conclusions may be drawn from present work, as:

1. The set up of data acquisition with strain gages through hole drilling method leads to map the residual stress with each layer of removed metal accurately .
2. The hole drilling method offers a uniform stripping rate, controlled temperature, a lack of machining stresses, and minimum handling to reduce errors which might occur due to stress relaxation and other changes in the stress pattern during material removal.
3. The strain distribution versus the hole depth depends on the specimen, which support the assumption of a nearly residual stress-free state. This phenomenon leads to the hypothesis that the residual stresses are generated by a constraint at a specimen height of 20 mm, based on the bonding of the sleeve and core material.
4. In the axial component compressive distribution of residual stress near the inner surface and is larger than the tensile distribution at the outer surface .
5. Product augmentation produces tensile residual stress pattern in radial , axial and tangential directions. radial and axial stress distributions with billet augmentation show tensile residual stresses near the die exit and compressive residual stresses in the rest of the product. Billet augmentation also results in compressive residual stresses in the tangential direction

9. REFERENCES

[1] Pratihar, S. Turski, M. Edwards, L. Bouchard, P.J. Neutron , "Diffraction Residual Stress Measurements in a 316L Stainless Steel Bead-on-Plate Weld Specimen". International Journal of Pressure Vessels and Piping 86 (2009) 13-19.

[2] Drew V. Nelson " Residual Stress Determination with Hole Drilling and Optical Methods ", Stanford University ,Proceedings of the SEM Annual Conference, June 1-4, 2009 Albuquerque New Mexico USA, Society for Experimental Mechanics ,2009.

[3] Mathar, J., "Determination of Initial Stress by Measuring the Deformations Around Drilled Holes", Transaction of ASME, Vol. 56, p.249, 1934.

[4] Jubing Chen , Yongsheng Peng and Shexu Zhao,"Hole-Drilling Method Using Grating Rosette And Moiré Interferometry", The Chinese Society of Theoretical and Applied Mechanics and Springer-Verlag GmbH 2009 (Acta Mech Sin (2009) 25:389-394)10 January 2009.

[5] ASTM Standard E837-02 , "Determining Residual Stresses by the Hole-Drilling Strain-Gage Method.", 2002.

[6] Abdullah Dhayea Assi, Mohsen J. Joaij, Moneer H. Tlafeh, Esam T. Abdullah, "The design and Manufacturing of a hydrostatic extrusion apparatus for Compound Cylinders from Al and Mg", Diyala Journal of Engineering Sciences , Vol. 6, No. 2, 2013, pp 86-103.

[7] Abdullah Dhayea Assi, Mohsen J. Joaij, Moneer H. Tlafeh, " Evaluation Of New Hypothetical Concept (LHSIR) for Die Profile Design for Hydrostatic Extrusion Of Al/Mg compound", Diyala Journal of Engineering Sciences , Vol. 7, No. 1, 2014, pp 40-61.

[8] Alfio Quarteroni and Fausto Saleri, "Scientific Computing with MATLAB and Octave" Second Edition, Springer-Verlag Italia, Milano, 2006.

Effect of Dipping Time and temperature on Produced Intermetallic Phases thickness in Hot Dip Galvanizing Process

BsC. Ruba Hussain Eleue ¹ , Asst. Prof. PhD. Bahaa S. Mahdi ²

^{1,2}Department of Production Engineering and Metallurgy, University of Technology

ABSTRACT

In this paper, hot dip galvanizing (HDG) process was studied to understand effect of dipping time and bath temperature on the growth and generation of produced intermetallic phases between Iron and zinc and the change or behavior in coating thickness at different immersion time and zinc bath temperature. Hot dip galvanizing specimens prepared at galvanizing temperatures in rang of 450 to 650°C in steps of 50°C and at different immersion time from (0.5 to 20) minutes. The specimens were characteristic by using scanning electron microscopy/energy dispersion spectroscopy.

KEYWORDS

Hot dip galvanizing, coating thickness, galvanizing temperatures, Electron microscopy, zinc coating

ARTICLE INFO

Received 1 November 2018

Accepted 22 December 2018

DOI: 10.xxxxx

ISSN: 2413-0230

AL-MUHANDIS Journal (JMISE)

© 2018 Iraqi Society of Engineers (ISE)

E-mail: jmise@ise-iq.org

Online: www.jmise.ise-iq.org

Office Address: Iraq, Baghdad, Al-Nidhal Q., 103-30-5

CORRESPONDING AUTHOR

Name: Ruba Hussien Elewe

Email: Ruba.Hussien2018@gmail.com

Research Field: metallurgy engineering

Google Scholar:

1. INTRODUCTION

The most common commercial processing technique used to protect steel components in corrosive environments is hot-dip galvanizing with various applications in iron and steel components [1].

This technique has been adopted as well proven feasible process since 1800 soon after the exploration of iron and zinc. The exploration of galvanizing goes back to 1742 when a French chemist named Melouin described in a presentation to the French Royal academy, a method of coating iron and steel parts with liquid zinc [2].

In hot-dip galvanizing process in the zinc melted bath, a Fe - Zn coating grows on galvanized parts as a result of rather complicated process of atomic diffusion of both metals with formation of elementary intermetallic bonds and subsequent phase transformations [3] [4].

These processes are running in the surface layer of galvanized metal, then on the interface of the surface of metal and melt of the zinc and finally in the actual melt close to the galvanized part. Depending on composition of the steel, temperature and composition of the electrolytic bath, thickness of the galvanized part, duration of the stay in the bath, surface condition and speed of cooling a coating is formed consisting of various intermetallic compounds of Fe - Zn [5].

Different composition and thicknesses consisted in Layers compounds. They are marked with a Greek alphabet letters, i.e. gamma (Γ), gamma1 (Γ_1), delta (δ), zeta (ζ), and eta (η). These phases differ significantly not only by composition but in morphology of the grain and also by mechanical characteristics [6] [7].

Formation of phases in the coating is based on the binary phase diagram Fe - Zn which shown in Figure 1 and Figure 2. The two diagrams indicate the details of the existence of individual intermetallic compounds, where the phases based on the diffusion processes [8].

In the following, some of the researches made by investigators and researchers to study hot-dip galvanizing process.

Peng Bicao (2008) studied the effects of Zn bath temperature on the hot-dip galvanizing coating where they were papered galvanizing samples at a temperature in the range of (450–530)°C. He found when galvanizing temperature was increased from about 450°C to 470°C; coating has a compact with coherent zeta phase on upper of delta phase.

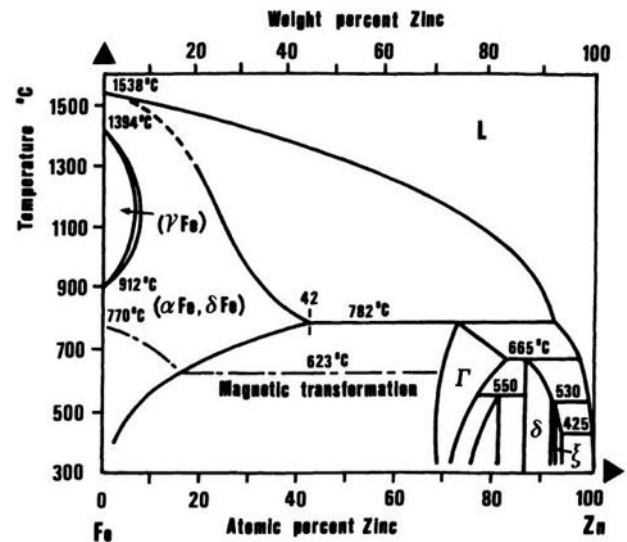


Figure (1): Phase diagram Fe - Zn [9]

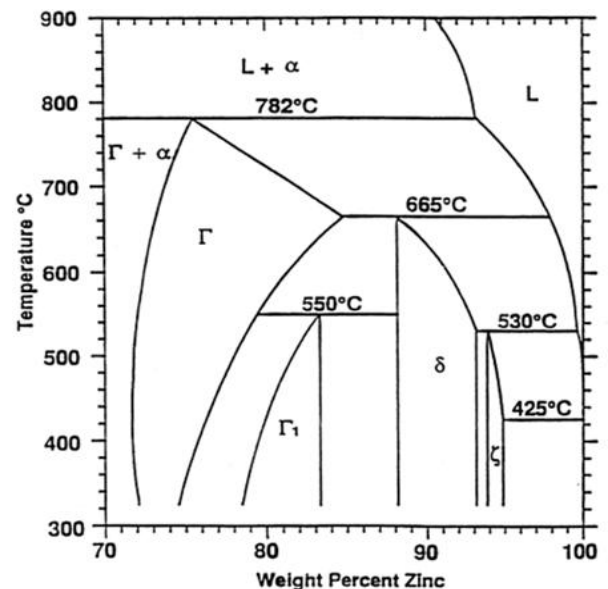


Figure (2): the Zinc rich section of the iron- zinc binary phase diagram [10]

The coating grows fastest at a temperature of about 480 °C in galvanizing at similar dipping times, where the coating thicknesses reach the maximum value at a temperature of about (530 °C).[11]

D. Kopyciński (2013) studied the intermetallic phases formation in hot dip galvanizing process. He described the mechanism of formation of the structure in protective coating, and the growth on Fe surface through hot-dip galvanizing. The first stage of the galvanizing process, directly after the Fe sample dipping in galvanizing bath, is the layer of frozen Zn crystallizing on sample surface. Subsequently, as a result of isothermal solidification, an alloyed layer of the coating; composed of the sub-layers of intermetallic Fe-Zn phases, is formed. At the initial stage of presence of alloyed layer, another layer that of

undercooled liquid, is formed on Fe surface dip in liquid Zn. As a result of peritectic reactions under metastable conditions, the individual phases are born, forming sub-layers in predictable sequence of Γ_1 , δ and ζ [12].

ChoukriLekbir (2017) studied the effect of galvanized dipping time and cooling environments on electrochemical corrosion performance of hot dipping galvanizing, In addition, he studied the evaluation of microstructure, structure and thickness of zinc coatings for various dipping times and also two cooling patterns (water and air). When the dipping time is longer, the coatings thickness increases more, and these characteristics become the better. When comparison between the two cooling environments it was found that the coatings of zinc formed by hot dipping galvanizing in air cooling modes offers a better protection to steel compared to corrosion than cooling by quenching in water which exhibited a brittle corrosion behavior because of the presence of cracks [13].

This work concentrates on the thickness of these intermetallic compounds according to the hot dip time and temperature variables. The thickness of these compounds is very important in the resulted product because the corrosion resistance and life span of the product depend directly on these layer properties.

Also, the mechanical surface properties affect the application where the product after galvanizing need more fabrication processes or not because thin sheet metals subjected to bend or cold formed favorite ductile coating layer therefore there are need to produce pure zinc coating layer instead of hard compounds which lead to cracks or scales and lose of coating at outer and inner corners. In other hand the phases represent good metallurgical bond needed to give better wear and scratch resistance.

2. EXPERIMENTAL

2.1 Variables:

Wide ranges of molten zinc bath temperatures chosen from 450 to 650°C with 50°C between each experiment. The dip time also begin from very short time of 30 second till 20 minutes gives wide spectrum to give a clear estimation for the resulted metallurgical changes. Table 1 show the number of experiments needed to complete the data about the effect of temperature and time on the resulted phases.

According to Table 1 there are needs to coating 35 steel specimens with changing the above variables.

Table (1): Hot dip galvanizing experiments numbers needed with changing dipping times and molten zinc bath temperatures.

Time (min.) \ Temp. (°C)	0.5	1	2	5	10	15	20
450	1	2	3	4	5	6	7
500	8	9	10	11	12	13	14
550	15	16	17	18	19	20	21
600	22	23	24	25	26	27	28
650	29	30	31	32	33	34	35

2.2 Materials:

Low carbon steel C1004 sheets with thickness of 1mm chosen as the galvanized material. Table 2 shows the chemical analysis done of C1004 steel. The steel sheet is divided to thirty-five specimens with dimensions of (80×10×1 mm). These specimens prepared by grinding up to 2000 grid using silicon carbide grinding paper.

Table (2): Chemical analyzes of steel specimens and the standard C1004 steel.

Name	C	Cr	Cu	Mn	Ni	P	S	Si
C1004	0.06	0.25	0.04	0.04	0.35
	max			max		max	max	max
Tested sheets	0.047	0.0153	0.032	0.199	0.0104	0.013	0.0175

2.3 Material Preparing

After grinding the steel strips immersed in 10% hydrochloric acid (2.8 molarity) for 4 minutes then washed by water well then again immersed in a solution of (50g zinc fluoride + 50g zinc chloride) in 300ml distilled water for 5 minutes and dried in hot air for 10 minutes before hot dip process. There is no need grease cleaning because any oil or grease not used in fabrication processes. The molten zinc bath consists of high purity zinc (99.99999 Zn %) melted in kettle in electric furnace [14] [15] [16].

2.4 Hot Dip Process:

Until the furnace temperature stables for the intended temperature the furnace door opened quickly and the surface of the molten zinc wiped from oxides then the steel strip immersed to depth of 60 mm in molten zinc. After waiting some time according to calculated dipping time furnace door opened with re-wiping the molten zinc surface and the steel strip is withdrawn

slowly. The galvanized steel strip was cooled in air. Figure 3 shows the completed galvanized specimens.



Figure (3): completed galvanized specimens

2.5 Testing:

After galvanizing process all specimens sliced as small parts with length of 1 centimeter then this small parts grouped together and mounted by acrylic epoxy as shown in Figure 4, to prepare for metallographic. In this way all the metallurgical aspects for specimens subjected to test by Scanning electron microscope (VEGA 3LM) assisted by EDS detector in Production and Metallurgy Engineering Dept., UOT, Baghdad.



Figure (4): steel sheets after cutting and mounting

3. RESULTS AND DISCUSSION

By gathering data from the Scanning electron microscope images for the micro structural galvanized sections as shown in (Figure 5, 6, 7, 8, 9), the thickness of intermetallic phases recorded and represented in Figure 10 and table 3 to identify the thicknesses of intermetallic phases with different dipping times and temperatures.

Table (3): the thicknesses of intermetallic phases with different dipping times and temperatures.

Bath Temp. °C	450	500	550	600	650
Time (min.)	Intermetallic layers thickness(μm)				
0.5	4	3.22	52.9	24.79	53.9
1	4.375	3.64	67.91	29.75	62.5
2	30.9	18.77	96.9	58.77	52
5	250	100	126.79	44.55	12.5
10	63.6	138.35	200.80	23.68	10.4
15	94.7	157.33	197.62	20.14	13.157
20	97.5	206.6	205	27.43	10

The dipping time plays the most effective factor, where at short dipping time about (0.5, 1) minutes the thickness of intermetallic layer is very small about ($\approx 4\mu\text{m}$) at 450°C compare with thickness when increasing dipping time to (2 minutes and above) which reach to about ($97\mu\text{m}$). Furthermore, increasing dipping time leads to increase in intermetallic layer thickness compounds, because of thicker layer related to increase the activity of diffusion depth of zinc atoms in steel surface with increasing time and generating more intermetallic phases thickness, while with short immersion time it is not enough diffused atoms of zinc to generate intermetallic phases as shown in Figure 5 in thirty second of immersion all the intermetallic phases represent the minimum values [17].

The diffusion process speed between solid steel surface and solid intermetallic phases is constant at a fixed temperature of (550°C), where at short immersion time, the transferred Iron atoms will be at low concentration in the layer which results in low concentration intermetallic compound such as (Zeta Phase), but with increasing the time the diffused iron atoms will be increased but the solidified galvanized layer will be thickened and behaves as an obstacle to allow Iron atoms to release in liquid Zinc. In this situation, the Iron atoms density will increase near steel surface, causing higher intermetallic phases such as (Gamma Phase)

When increasing the temperature to 600 and 650°C , there is a notable decrease in the intermetallic layer thickness. At the Iron-Zinc equilibrium diagram in the rich zinc region (Figure 2) it can be seen that the zeta and delta phases in the liquid-solid region at temperature above 530°C , then at immersion these phases in the semi-solid state at immersion position and when the sheet is withdrawn from the bath portion of the semi-solid phases remain in the bath and there is some loss of coating layer. Also, at this high temperature the ability of molten zinc to dissolve the generated phases is high, leading to a decrease in the thickness of the intermetallic phases layer. The generated phases will be dissolved again in

molten zinc, where the molten zinc will penetrate the phases at grain boundaries as shown in Figure 9 at temperature of 650°C with immersion time of five minutes and above and finally will separate the phases grains which migrates far of surface toward molten zinc and dissolved there which cause decrease in bath zinc purity.

From the Figure 10 which represents graphically behavior of increasing and decreasing intermetallic phases for all experiments, the maximum thickness of intermetallic phases can be obtained in temperature range from 550 to 500°C and minimum values were at temperature above 600°C. While 450°C of the bath temperature gives an average value of these phases.

4. CONCLUSION

- 1- In hot dip batch galvanizing process at low temperatures (450 to 550)°C, increasing dipping time leads to thick the galvanizing layer.

- 2- At 600°C and above for molten zinc bath, the thickness of galvanized layer decreased dramatically compared to low galvanizing temperature.
- 3- In high galvanizing temperatures, increasing immersion time does not help in increasing coating thickness, but it may decrease coating layer due to dissolving of Iron in Zinc generating phases and making most of coating layer compound of complex phases from Iron and zinc instead of pure zinc layer.
- 4- In immersion time of thirty seconds, one, two and five minutes Delta, Zeta and Eta phases were found, while after two minutes Eta phase beings to be eliminated.
- 5- For immersion times of (10, 15, and 20) minutes, four layer formation Eta, Zeta Delta and gamma phase begin to appear in thin layer attached to steel surface.

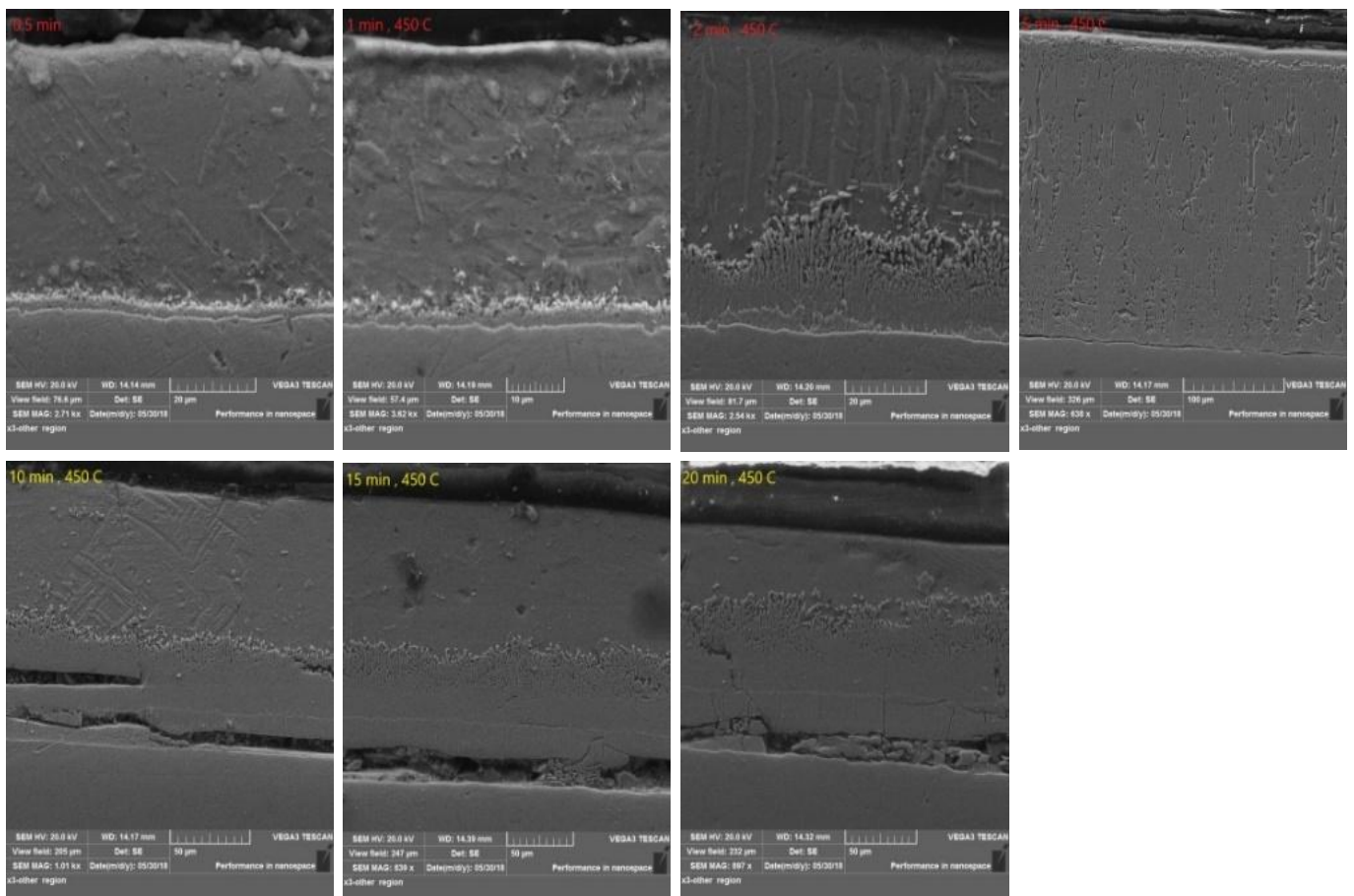


Figure (5): Micro-structural SEM images for galvanized sections for (450°C) at different immersion times.

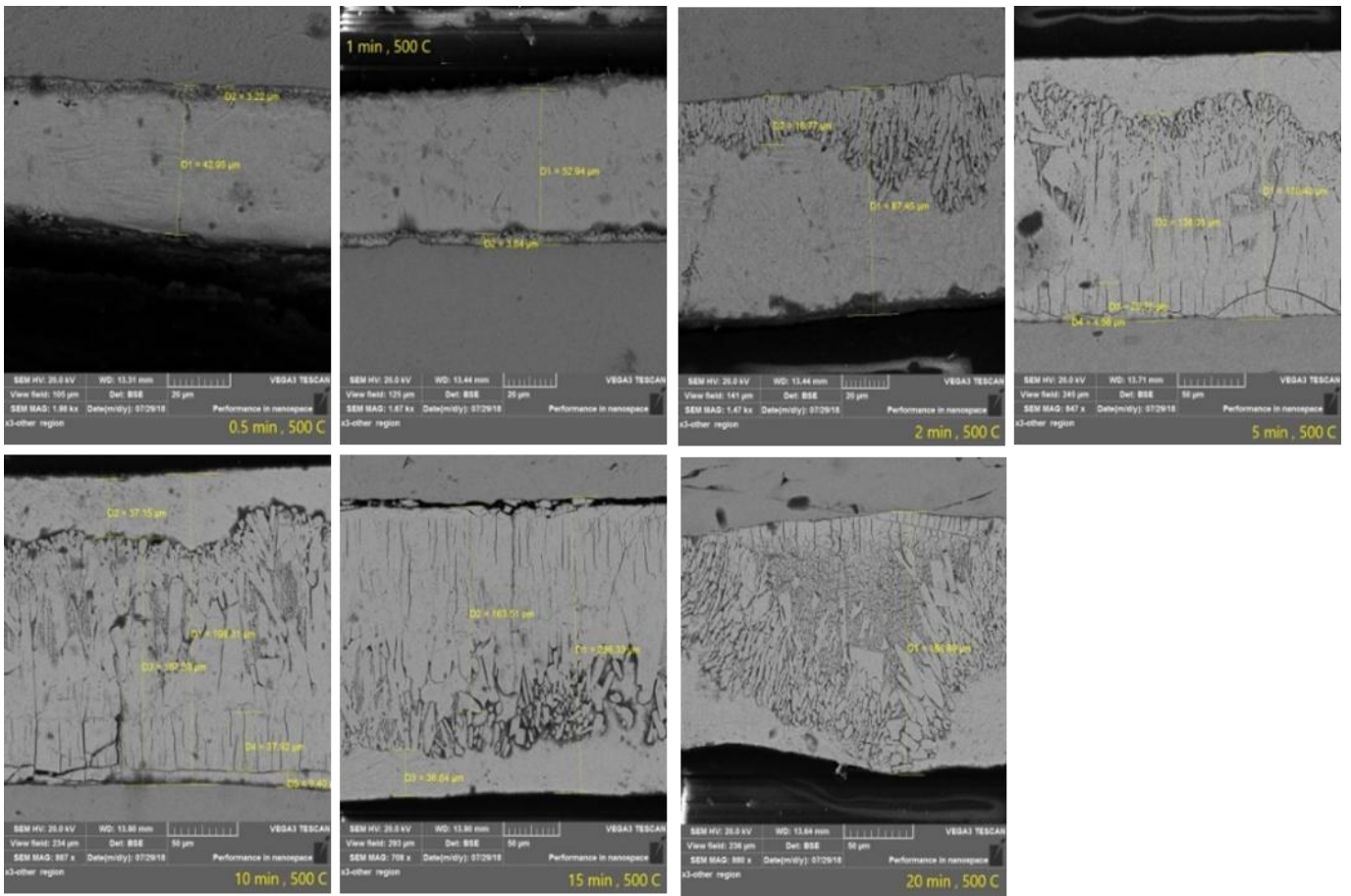


Figure (6): Micro-structural SEM images for galvanized sections for (500°C) at different immersion times.

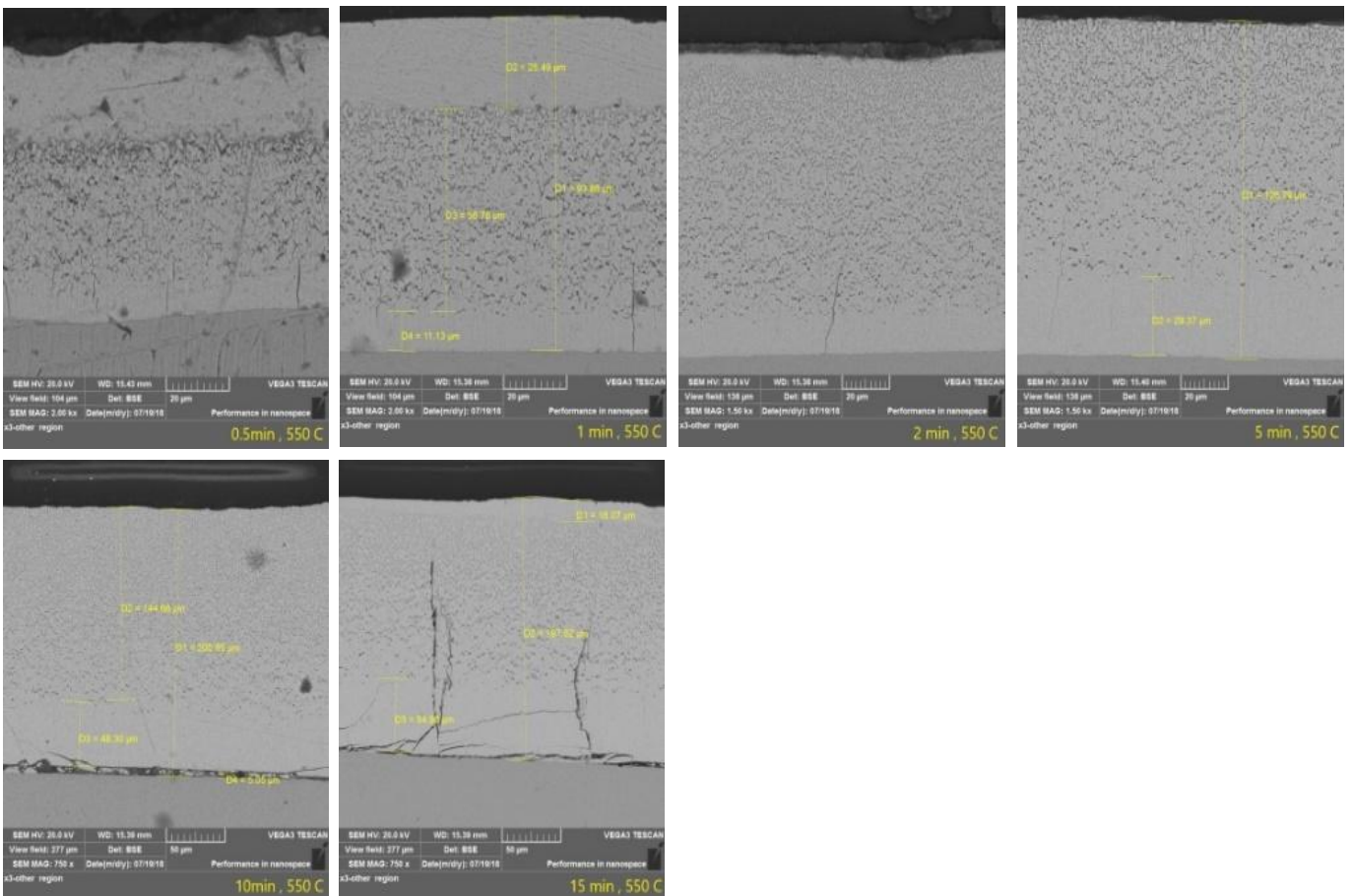


Figure (7): Micro-structural SEM images for galvanized sections for (550°C) at different immersion times.

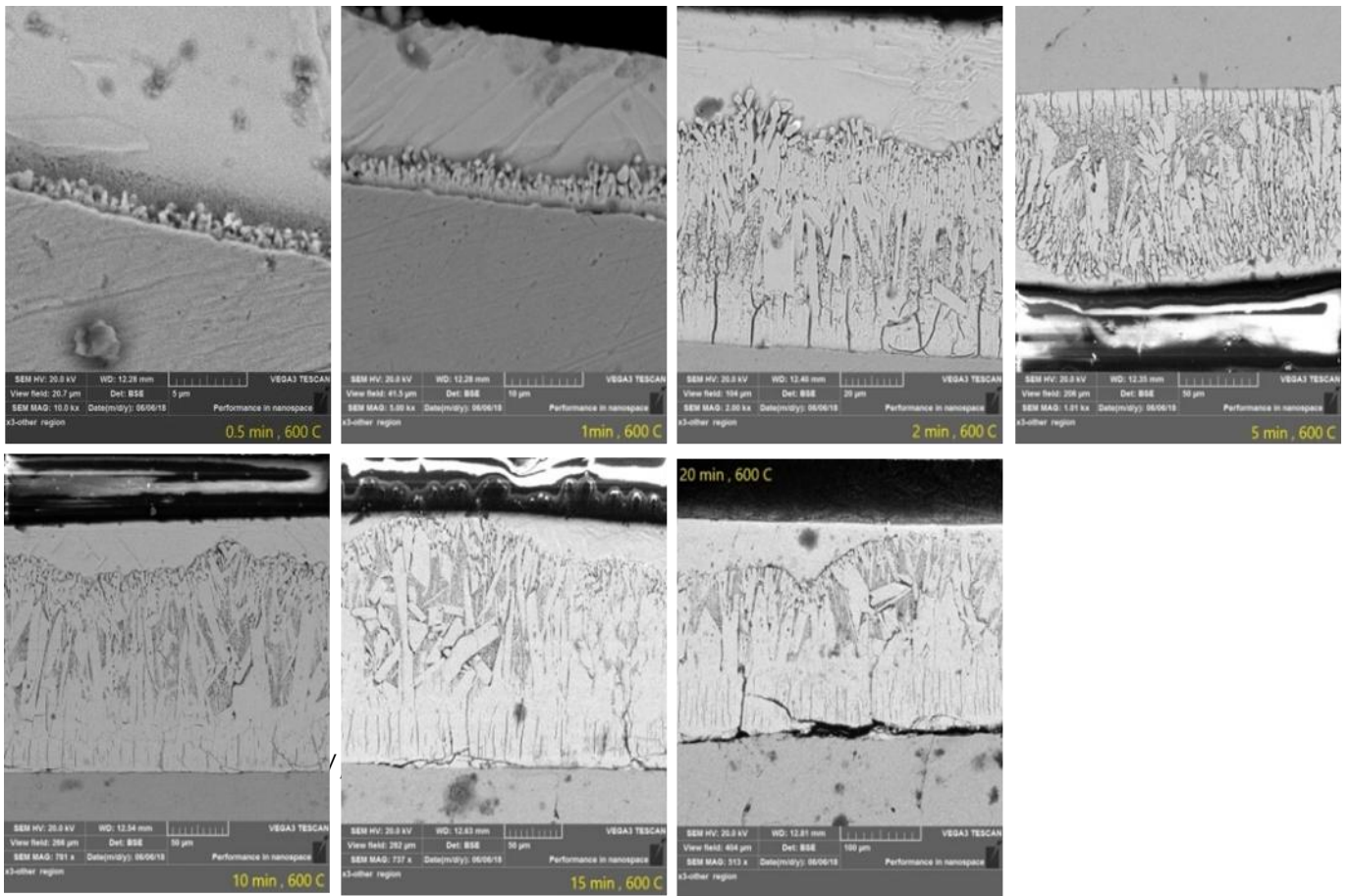


Figure (8): Micro-structural SEM images for galvanized sections for (600°C) at different immersion times

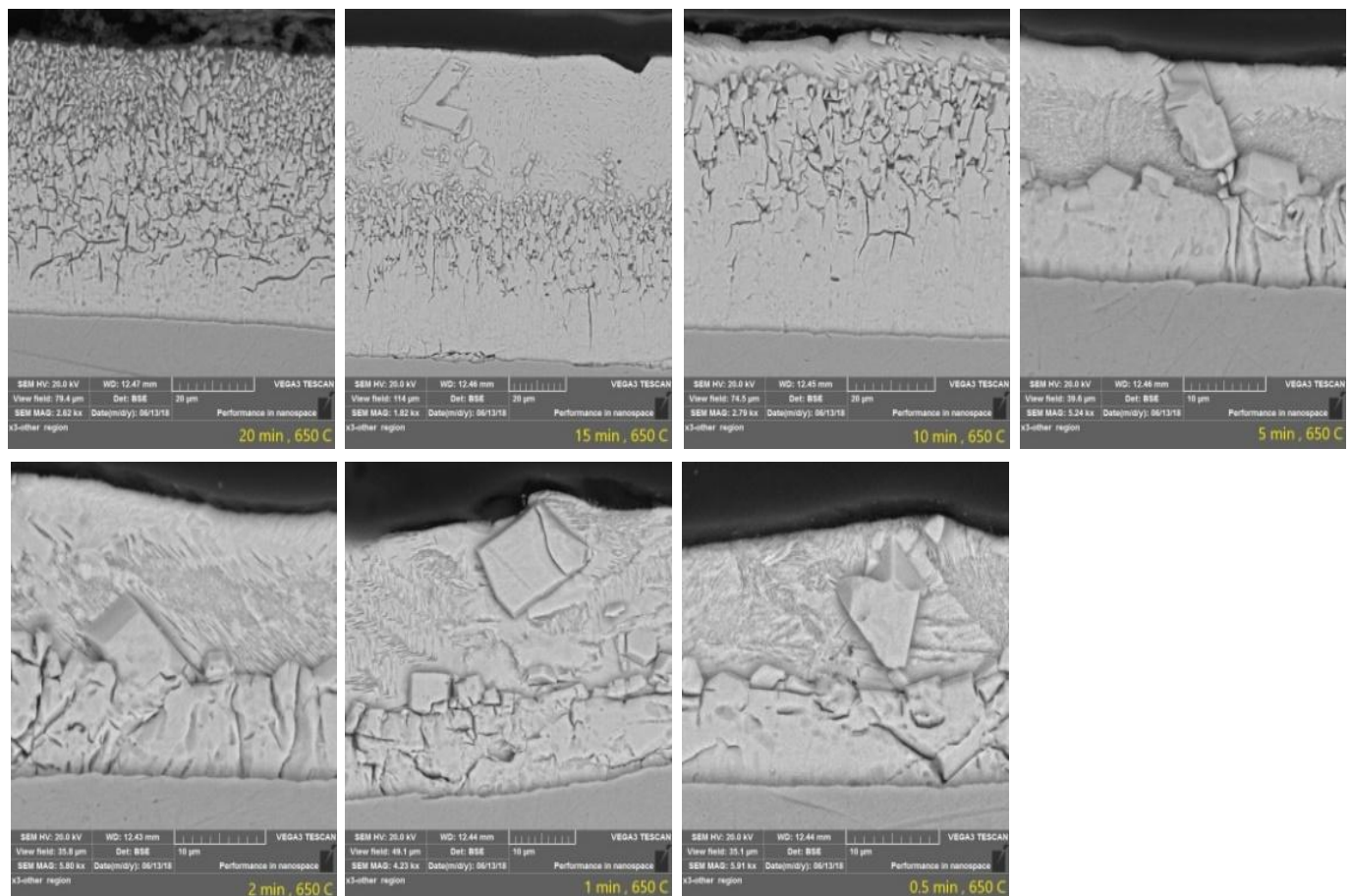


Figure (9): Micro-structural SEM images for galvanized sections for (650 °C) at different immersion times.

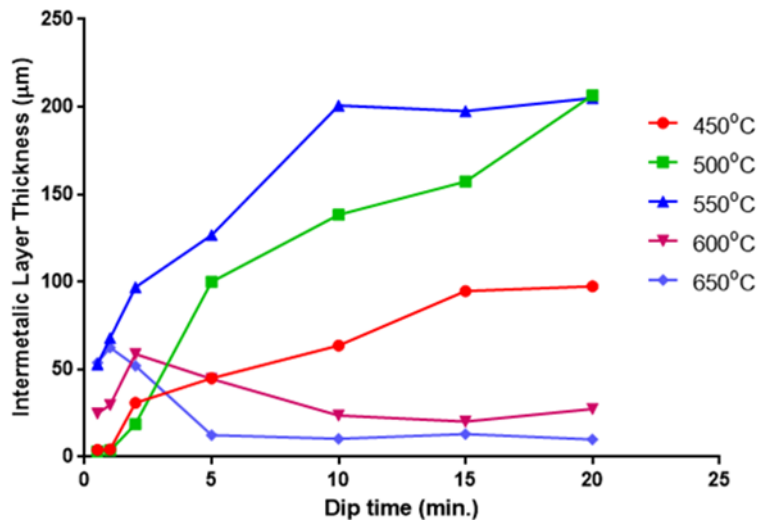


Figure (10): Intermetallic layer thickness change with different dipping time at various bath temperatures.

5. REFERENCES

- [1] Lamia Darsouni, Mohamed Zine Touhami, Abdelkader Khettache, Omar Benchiheub, "Surface Characteristics Analysis and Adherence Evaluation of Hot-Dip Galvanized Low Alloy Steel" *Synthèse: Revue Sciences Technologie* Vol 36.1, P177-189, (2018).
- [2] Maaß, Peter, and Peter Peißker, Eds. "Handbook of Hot-Dip Galvanization", John Wiley & Sons, (2011).
- [3] T.J. Langill, *Batch Process Hot Dip Galvanizing, Corrosion: Fundamentals, Testing, and Protection*, Vol 13A, ASM Handbook, P 794-802, (2003).
- [4] S.M.A. Shibli, "A Review on Recent Approaches in the Field of Hot Dip Zinc Galvanizing Process", *Surface & Coatings Technology*, P1-20, (2014).
- [5] J.D. Culcasi, "Control of the Growth of Zinc-Iron Phases in the Hot-Dip Galvanizing Process", *Elsevier, Surface and Coatings Technology*, Vol 122, P 1-23, (1999).
- [6] Han, K., Ohnuma, I., Okuda, K., & Kainuma, R. "Experimental Determination of Phase Diagram in the Zn-Fe Binary System" *Journal of Alloys and Compounds*, Vol 737, P 490-504, (2018).
- [7] P. Pokorny, "Description of Structure of Fe-Zn Intermetallic Compounds Present in Hot-Dip Galvanized Coatings on Steel", *Metalurgija*, Vol 54, P 707-710, (2015).
- [8] A.R. Marder, "The Metallurgy of Zinc-Coated Steel", *Progress in Materials Science* 45, Pergamon, P191-271, (2000).
- [9] Lazik, S., C. Esling, and J. Wegria, "Cracking in Zinc Layers on Continuous Galvanized Sheets: a Review " *Texture, Stress, and Microstructure*, Vol 23.3, P 131-147, (1995).
- [10] Massalski, T. B, "Phase Diagrams" *ASM Metals Handbook*, (1992).
- [11] Peng Bicao, "Effects of Zinc Bath Temperature on the Coatings of Hot-Dip Galvanizing", *Surface & Coatings Technology*, Vol 202, Elsevier, P1785-1788, (2008).
- [12] Kopyciński, Dariusz, and Edward Guvzik, "Intermetallic Phases Formation in Hot Dip Galvanizing Process", *Solid State Phenomena*, Vol. 197, Trans Tech Publications, (2013).
- [13] Choukri Lekbir, "Effect of Immersion Time and Cooling Mode on the Electrochemical Behavior of Hot-Dip Galvanized Steel in Sulfuric Acid Medium", *Journal of Materials Engineering and Performance*, P1-10, (2017).
- [14] Malone, John F. "Painting Hot Dip Galvanized Steel" *Materials Performance*, Vol 31.5, P 39-42, (1992).

- [15] Vourlias, G., Pistofidis, N., Stergioudis, G., Pavlidou, E., & Tsipas, D "Influence of Alloying Elements on the Structure and Corrosion Resistance of Galvanized Coatings." *Physica Status Solidi (a)* Vol 201.7, P 1518-1527, (2004).
- [16] Sultan, Abdullah Emad "Alternative Methods for Sealing Overlapping Steel Members with Narrow Gaps during Galvanizing" Diss. Virginia Tech, (2018).
- [17] G.K. Mandal¹ , D. Mandal¹ , S.K. Das¹ , R. Balasubramaniam² and S.P. Mehrotra¹, "Microstructural study of galvanized coatings formed in pure as well as commercial grade zinc baths", *Transactions of the Indian Institute of Metals* Vol 62.1, p 35-40, (2009).

ACKNOWLEDGMENT

I wish to express my sincere thanks and deepest gratitude to my supervisor Dr. Bahaa Sami and I offer sincere thanks to my family: Mother, father for their continuous supports and encouragements, friendly attitudes and their endless love to achieve my goals at every stage of my life.